University Mohamed Khider of Biskra
Faculty of Fundamental Sciences, Nature and Life Science
Department of Matter Sciences

MASTER DISSERTATION

Matter Sciences
Physics
Energetics and Renewable Energies

Ref. :

Presented and defended by :
Guettiani Nour El Houda **Youcef Kawther**

25-09-2020

Modeling and ab initio simulation of the adhesion of aluminum to copper oxide

---

Jury :

Mr	Nouredine Sengouga	Professor	University of Biskra	President
Mr	Abdelouahab Ouahab	Professor	University of Biskra	Supervisor
Mr	Rami Boumaaraf	M.C. B	University of Biskra	Examiner

Année universitaire : 2019-2020

Acknowledgment

We thank God the Almighty for giving us the privilege and the chance to study and follow the path of science and knowledge.We extend our sincere thanks to our supervisor Mr. Ouahab Abdelouahab for his understanding and advices and his invaluable help, for his kindness and his efficient guidance.

We also extend our deep gratitude to all the professors of Mohamed Khaider University, in particular those of the Seience of Mattere department. Finally, we would like to thank all the people, from near or far, who contributed to the development of this brief.

To our comrades and friends with whom we shared the best moments during our studies, but also the most difficult moments, which they helped us to overcome.

we address our most sincere thanks to our dear parents, to whom our gratitude is immeasurable, and to all our families.

Dedicate

* To our mothers the light of our eyes: our fathers, our life.

* our dear brothers And our dear sisters .

* To all our friends, especially our dear Chaima and Lynda .

* Lastly, We offer this memoir to all our families: old and young.

* To all the readers of our memoir.

Contents

Chapter III: Results and discussions.

	List of Figures	
	Title	**Page**
Chapter I	**Fig I.1:** Powder of Cu_2O	3
	Fig I.2: Crystal structure of Cu_2O	4
	Fig I.3: Powder of CuO	6
	Fig I.4: Crystal structure of CuO	7
	Fig I.5: Natural Cu_4O_3 forme	9
	Fig I.6: Ball and stick model of paramelaconite Cu_4O_3 with body-centered tetragonal lattice. Both conventional cell (left panel) and primitive cell (right panel) are shown.	10
	Fig I.7: Aluminum "Al".	12
	Fig I.8: (a). The fcc crystal structure of Aluminum direction with <001>. pointing up exposes the ABCABCA stacking of close packed atoms. **(b).** crystal structure of Al. **(c).** Primary cell of Al	13
	Fig I.9: (a). The fcc crystal structure of Aluminum direction with <111>. **(b).** Aluminum in direction x. **(c).** Aluminum in direction y. **(d).** Aluminum in direction z.	14
Chapter II	**Fig II.1:** Flowchart representing the principle of solving Kohn-Sham's equations by diagonalization of the Hamiltonian matrix.	30
	Fig II.2: Illustration schematizes the potential of all-electron (solid lines), pseudo-electron (broken lines) and their corresponding wave functions .	32
Chapter III	**Fig III.1**: The total energy of Al mesh as a function of the number of points K .	40
	Fig III.2: The total energy of Cu_2O as a function of the number of points K.	40
	Fig III.3: The total energy of Al mesh as a function of E_{cut}.	41
	Fig III.4: The total Energy of Cu_2O mesh as a function of energy $E_{cut\text{-}off}$.	42
	Fig III.5: The total Energy of Al as a function of the lattice parameter of Al.	43
	Fig III.6: The total Energy of Cu_2O as a function of the lattice parameter of Cu_2O.	43
	Fig III.7: Total energy as a function of volume for Al.	44
	Fig III.8: Total energy as a function of volume for Cu_2O.	45
	Fig III.9: An illustration of the expansion in the studied material.	46
	Fig III.10: Mismatch of $AlCu_2O$ in direction <001>.	47

GENERAL Intoduction

General introduction

The interest in the knowledge of surfaces and interfaces derives as much from the desire to understand fundamental problems as from the practical importance of their structures. Indeed, the development and study of thin films, surfaces and interfaces are a very important axis both from a fundamental point of view in materials sciences, as technological for various sectors of industry. Any solid is limited by surfaces that are in contact with a vacuum or with some other material. The existence of many practical applications of metals depend on the state of their surfaces and the properties thereof (catalysis, semiconductors, anti-corrosion deposits, anti-wear deposits,...). Recent technological advances have made it possible to develop and control the growth of interfaces.

Nowadays you can make materials with new properties that are not found in nature. It is a question of describing the materials by theoretical models which can explain the experimental observations, and especially to carry out modeling or "virtual experiments" and predicting the behavior of materials and the way they adhere to each other, which have not yet been designed due to the cost and difficulty of that and also allows us to know the directions and the number of layers for good adhesion. Thus, the interest of modeling and simulation is to study the various possibilities that present themselves, and to guide the industry towards the best choices with minimum cost.

When we study the adhesion of a layer on a surface, we are interested in several details: the geometry, the length of the chemical bonds with the surface atoms, the type of chemical bond that is established. The question that arises, is there an adhesion between the copper oxide layer and the aluminum?

To perform these calculations, we used the ab-initio calculation code based on the pseudopotentials and plane waves method using qauntum espresso and SIESTA code. We have described the effects of exchange and correlation by the generalized gradient approximation (GGA) and limiting the study to the two interfaces Al(001)/Cu2O and Al(111)/Cu2O. This memoire consists of three chapters in addition to an introduction and a general conclusion.

In the first chapter we present generalities to the materials of the compound to be studied represented in aluminum and copper oxide of all kinds while recalling the physical and electronic and structural properties (which we need in what follows in our calculations).

In the second chapter we give a brief overview on the establishment of the density functional theory as it can be used to describe the interactions between materials. It also give

access to the total energy of the system as well as to its electronic structure, and we will end by giving an overview of the codes used during our work.

The third chapter is divided into three parts, the first part will be devoted to the study of the structural properties of the materials and the calculations to estimate the cut-off energy and the number of k-points needed to proceed and then unit cell parameters of both the metal and the oxide which are essential to create the right the shape of the simulation box, then the second part will study the adhesion of the copper oxide layer on the aluminum, while the last part will be to analyze the electronic properties (PDOS) and interpret the results.

Finally, we will end with a general conclusion which brings together all the main results of this work.

Chapter I:

Bibliographic studies

I-Introduction:

Copper oxides are one of the most important semiconductor oxides as they are compounds that have perfect properties that allow them to be used in a variety of applications, especially thin films. Aluminum owing to the vertus such as earth-abundant and cost effective has been regarded as a promising material for many applications. In this chapter we will present some generalities about the two materials used in thesis our there are three types of copper oxides and aluminum.

II. Cuprite Oxide Cu_2O:

The name “cuprites” of cuprous oxide Cu_2O comes from the Latin “cuprum”, meaning copper. Old miners used to call it “ruby copper”. Cuprites’ mineral has been a major ore of copper and is still mined in many places around the world. Cuprites’ color is red to a deep red that can appear almost black. Dark crystals show internal reflections of the true deep red inside the almost black crystal. New applications of Cu_2O in nanoelectronics, spintronics, and photovoltaic’s are emerging [1].

Fig I.1: Powder of Cu_2O.

II.1: Structural characteristics of Cu_2O:

Cuprites crystallizes in a simple cubic structure which can be viewed as two sub lattices, a face centered cubic (fcc) sub lattice of copper cations and a body-centered cubic (BCC) sub lattice of oxygen anions. The oxygen atoms occupy tetrahedral interstitial positions reltive to the copper sub lattice, so that oxygen is tetrahedrally coordinated by copper, whereas copper is linearly coordinated by two neighboring oxygen’s [1], see Fig I.2.

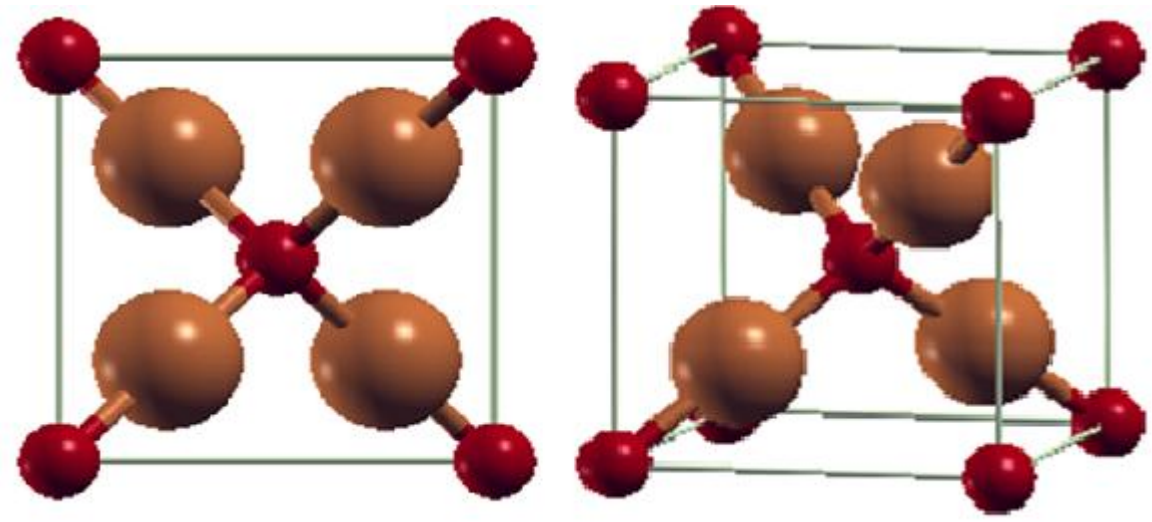

Fig I.2: Crystal structure of Cu_2O.

Cuprite Oxide Cu_2O		
Crystal System		Cubic
Space group		$Pn\bar{3}m$
Unit cell (Å)		a = 4.2696
Distances	**Cu-O**	1.84 Å
	O-O	3.68 Å
	Cu-Cu	3.02 Å

Table I.1: Crystal structural properties of Cu_2O [1].

II.2. Physical properties of Cu_2O:

Cu_2O is a semiconductor material with p-type conductivity and a band gap of 2.1 eV [2], it does not dissolve in water [3], is widely used in numerous implementations due to high absorption coefficient, excellent visible light photo catalysis properties and high performance solar energy conversion [4-5], it can be prepared by thermal oxidation [6], by anodic oxidation [7], by spraying [8] and by electrochemical deposition [9]. The electrical properties of cuprous

oxide films vary considerably with the preparation methods, which result from the large variation in the resistivity of Cu_2O films [10].

In addition, it has interesting properties such as a rich exciton structure, which allows the observation of a well defined series of excitonic characteristics in the spectrum absorption and photoluminescence of bulk Cu_2O [3], Cu_2O has conduction and valence band capable of reducing and oxidizing water into hydrogen and oxygen [11].

Cuprite Oxide Cu_2O	
Density (g.cm-3)	6.106
Volume (Å3)	77.83
Molar volume (cm3.mol-1)	23.44
Molecular weight	143.092 g/mol
Fusion point	1235 °C
Relative permittivity	7.5
Band energy prohibited at room temperature	Eg= 2.09 Ev
Specific thermal capacity	Cp=70J/(K.Mol)
Thermal conductivity (k)	5.5 W/(K m)
Thermal diffusivity (α)	0.015 cm2/s

Table I.2: Physical properties of Cu_2O [3].

II.3. Oxidation of copper to Cu_2O:

Copper oxidizes to Cu_2O in air between 170 and 200 ° C [12-13]. The cuprite phase thus obtained strongly depends on the temperature and the partial oxygen pressure [14]. When copper oxidizes to Cu_2O, there is a modification of the structure, the insertion of oxygen and the reorganization of the copper atoms leads to an expansion of + 65% in molar volume. This change in volume can generate porosities or defects in the microstructure of the materials [15].

III. Cupric Oxide CuO:

Known as Copper oxide (secondary copper mineral) is a chemical compound of the formula CuO, this compound is known as tenorite under a mineral form which is black powder Fig I.3 a rare earth metal and the most stable form of oxidized copper. We have many methods can be used to prepare cupric oxide such as thermal oxidation, sintering, precipitation, spraying and electrochemical deposition [16]. And most of its applications are done in: Superconductor at high temperature, solar cells, gas capture magnetic holders, variances and catalysis, antimicrobial activity, photo electrochemical cells and batteries [17].

Fig I.3: Powder of CuO.

III.1. Structural characteristics of CuO:

Cupric oxide forms a much more complicated tenorite crystal. The monoclinic mesh contains four CuO molecules. These network constants are: a = 0.47 nm, b = 0,34nm ,c = 0,51nm et ß = 99,54º [19], the CuO belongs to the monoclinic crystal system, with a crystallographic point group of 2/m or C2/c [18], this mesh contains Cu^{2+} ions coordinated by four (4) O^{2-} ions in an approximately square planar configuration [19].

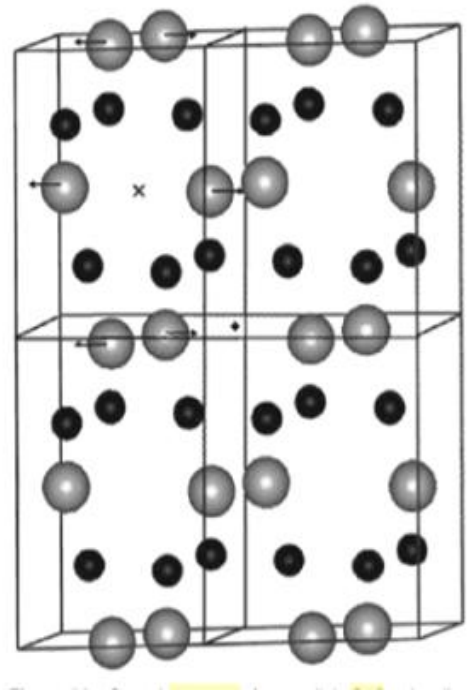

Fig I.4: Crystal structure of CuO.

(The gray spheres represent the Cu^{2+} ions and the black spheres represent the O^{2+} ions)

Cupric oxide CuO		
Crystal System		Monoclinic
Space group		C2/c
Unit cell		a = 4.6837 Å,b = 3.4226 Å ,c = 5.1288 Å β = 99.548° α = ɤ = 90°
Cell volume in		81.08 Å
Cell volume in u.a		4 [CuO]
Distances	Cu-O	1.96 Å
	O-O	2.62 Å
	Cu-Cu	2.90 Å

Table I.3: Crystal structural properties of CuO [17,21].

III.2. Physical properties of CuO:

CuO has attracted considerable attention because of its special properties, copper oxide used as a base material in high temperature superconductors as the superconductivity in these materials is associated with Cu-O bonds, as a p-type semiconductor CuO has a direct band gap of around 1.2 eV [19].

CuO is also used as standard material in the study of the understanding of physical properties different from that of the solid mass, properties generated by the transformation of the morphology mainly due to the reduction of the size, thus there exist various methods of synthesis of achieve nanometric size, the difference in the synthesis processes lies in the means of controlling the size and shape of the nanostructured material prepared [19].

Cupric oxide CuO	
Chemical name	Copper oxide
Other names	Copper monoxide Cupric oxide Oxocopper
Chemical formula	CuO
Volumic mass	6.505 g.cm^{3-}
Density	6.32g/cm^3
Band energy prohibited at room temperature (Eg)	1.2ev
Fusion point	1134°C
Boiling point	2000°C
Formula weight	79.57 g/mol
Solubility	**- Insoluble in:** water – alcohol – ammonium hydroxide -ammonium carbonate **- Soluble in**: ammonium – chloride – potassium cyanide
Relative dielectric constant	12
Magnetic susceptibility	χ = 239.10-6 cm3/mol
Refractive index	n_D = 2.63

Table I.4: Physical properties of CuO [23, 24,25].

III.3. Cu_2O to CuO oxidation:

CuO is obtained by the oxidation of Cu_2O from 300°C [11, 12]. CuO is always formed by oxidation of Cu_2O and never by direct oxidation of metallic copper. There is thermodynamically an impossibility of coexistence of copper with CuO, because whatever the temperature, the enthalpy of formation of Cu_2O is always lower than the enthalpy of formation of CuO. There is no intersection between the two curves of ΔG° [14]. The only observable systems are therefore copper and Cu_2O, and Cu_2O with CuO[22, 24].

IV.Paramelaconite Cu_4O_3 :

Paramelaconite is a natural, and very scarce mineral, it was first described by Koenig (1891), and more completely by Frondel (1941) [24]. The synthesis of bulk Cu_4O_3 through the conventional chemical routes is rather challenging, because it is very difficult to stabilize the Cu2+ and Cu+ ions simultaneously [25]. One of the versatile techniques to control the oxygen and the reaction (plasma) energy is the reactive DC magnetron sputtering technique [26, 27].

Fig I.5: Natural Cu_4O_3 forme.

IV.1. Structural characteristics of Cu_4O_3:

Paramelaconite is an oxide of copper intermediate between Cu_2O and CuO , has mixed valency, with half of the Cu ions formally in the +1, and the other half in the +2 oxidation state , its crystal structure (space group I41/amd) is built of inter-penetrating chains of Cu^{+}–O and Cu^{2+}–O[25]. The Cu^{2+} ions are planar coordinated to four O^{2-} ions, a three-dimensional Patterson synthesis led directly to placing copper atoms in 8c and 8d and oxygen in 4a and 8e: (0 l/4 z) etc, with z = 0.12 A [28]. See Table.I.5.

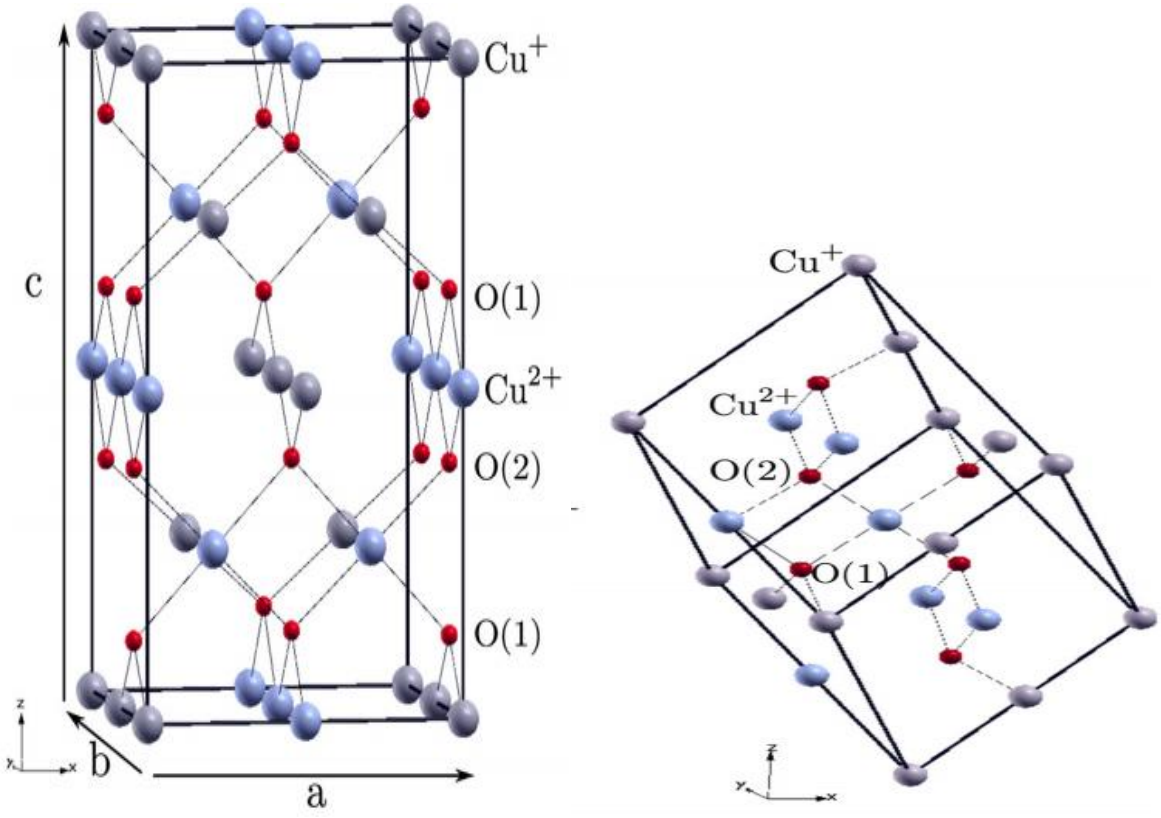

Fig I.6: Ball and stick model of paramelaconite Cu_4O_3 with body-centered tetragonal lattice. Both conventional cell (left panel) and primitive cell (right panel) are shown [28]**.**

Paramelaconite Cu_4O_3	
Crystal System	Tetragonal
Space group	I41/amd
Unite cell	a (Å)= 5.837, c (Å) =9.932, z (c)= 0.12
Ce11 volume	338 A^3
Z	4
Atom coordinates	Cu(1) 8c X=0 Y=0 Z=0 Cu(2) 8d X= 0 Y= 0 Z=1/2 O (1) 8e X=0 Y=1/4 Z=0.1173 O(2) 4a X= 0 Y=1/4 Z=3/8

Table I.5: Crystal structural properties of Cu_4O_3 [24].

IV.2. Physical properties of Cu_4O_3:

Cu_4O_3 is shown as an insulator [10], and thin films of this metal (of thickness 265 ± 5 nm) are p-type semi-conductors (hole density 2.4 × 1018 cc−1 and Hall mobility 0.04 cm2 V−1 s−1) and show a low resistivity (55 Ω cm). They have a direct band gap of 2.34 eV and an indirect band gap of 1.50 eV [27], Cu_4O_3 is good potential catalyst for oxidation [28]. An exact value of the energy gap in Cu_4O_3 is not known [29].

Paramelaconite Cu_4O_3	
Molar mass	302.18g/mol
Density	5.93g/cm^3
Number of variables	21
Unit cell volume	3.38 * 10–28 m3

Table I.6: Physical properties of Cu_4O_3 [32].

V. Aluminum “Al”:

The name aluminum is derived from the ancient name for alum (potassium aluminum sulphate), Al is a gray white metal, because of a thin layer of oxidation that forms quickly when it is exposed to air Fig I.7.

The aluminum component is present in the earth's crust [30], it represents almost 8% of the composition of the lithosphere after oxygen (42%) and silicon (28%) [32], which is incorporated into mineral bauxite ore and is in the form of aluminum oxide (alumina Al2O3: is a brittle, ceramic material that has a very high melting point of 1.773°C), and requires a large amount of energy to extract aluminum from its ore, it contains a low level of impurities, usually much less than 1% [30], very reactive metal [32], light in weight (2.700 kg.m-3) and melts at 660°C, and is very rare in its free form [30], the most important applications of Al: aerospace, aeronautics, automotive, cables electrical, food, nuclear reactors and building [31].

Fig I.7: Aluminum"Al".

V.1. Structural characteristics of Al:

Aluminum in its pure form has a face centred cubic crystal structure (fcc), with coordination number 12 and four atoms to the unit cell [32], which is a close-packed arrangement (the densest geometric packing of spheres attainable) with a layer sequence of ABCABCA… . This is illustrated in Fig.I.8 bellow [34].

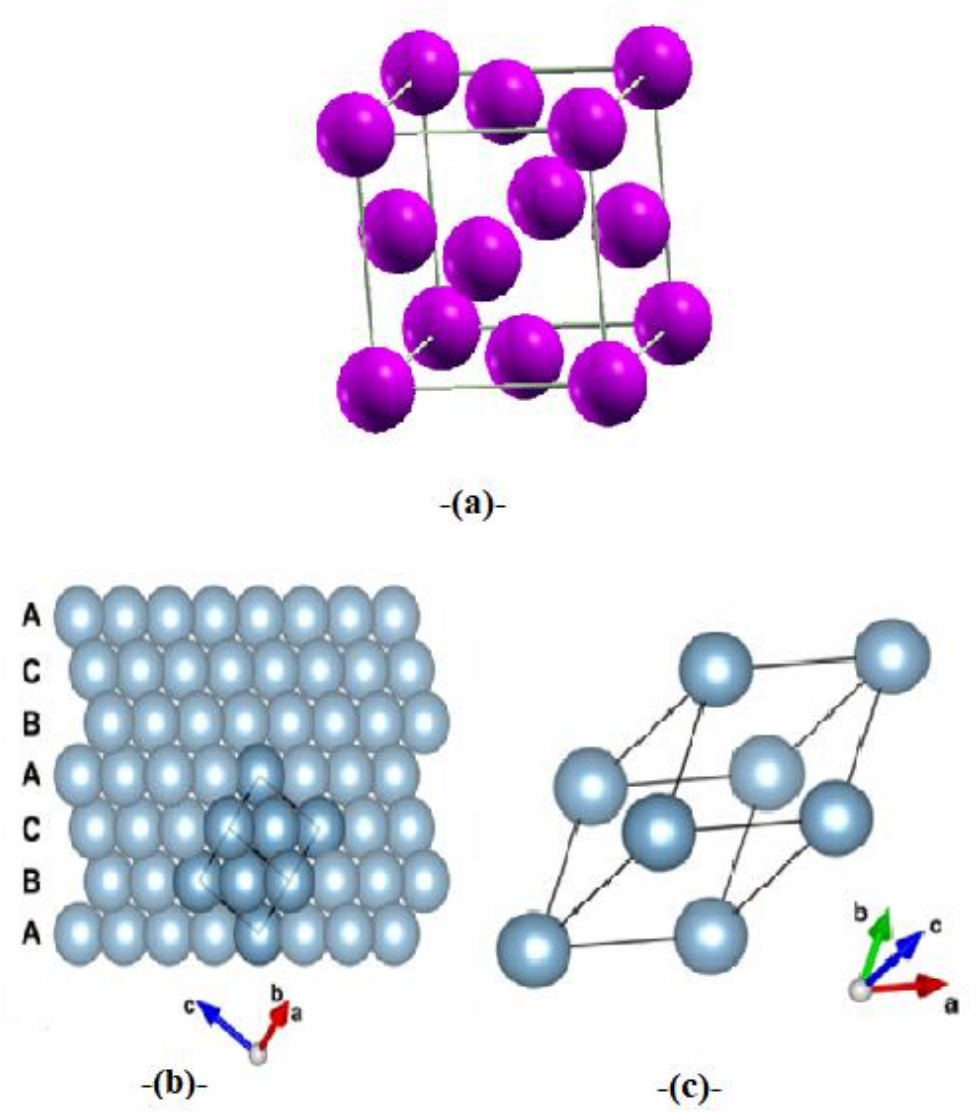

Fig I.8: (a). Crystal structure of Al. **(b).** The fcc crystal structure of Aluminum direction with <001> pointing up exposes the ABCABCA stacking of close packed atoms. **(c).** Primary cell of Al [32].

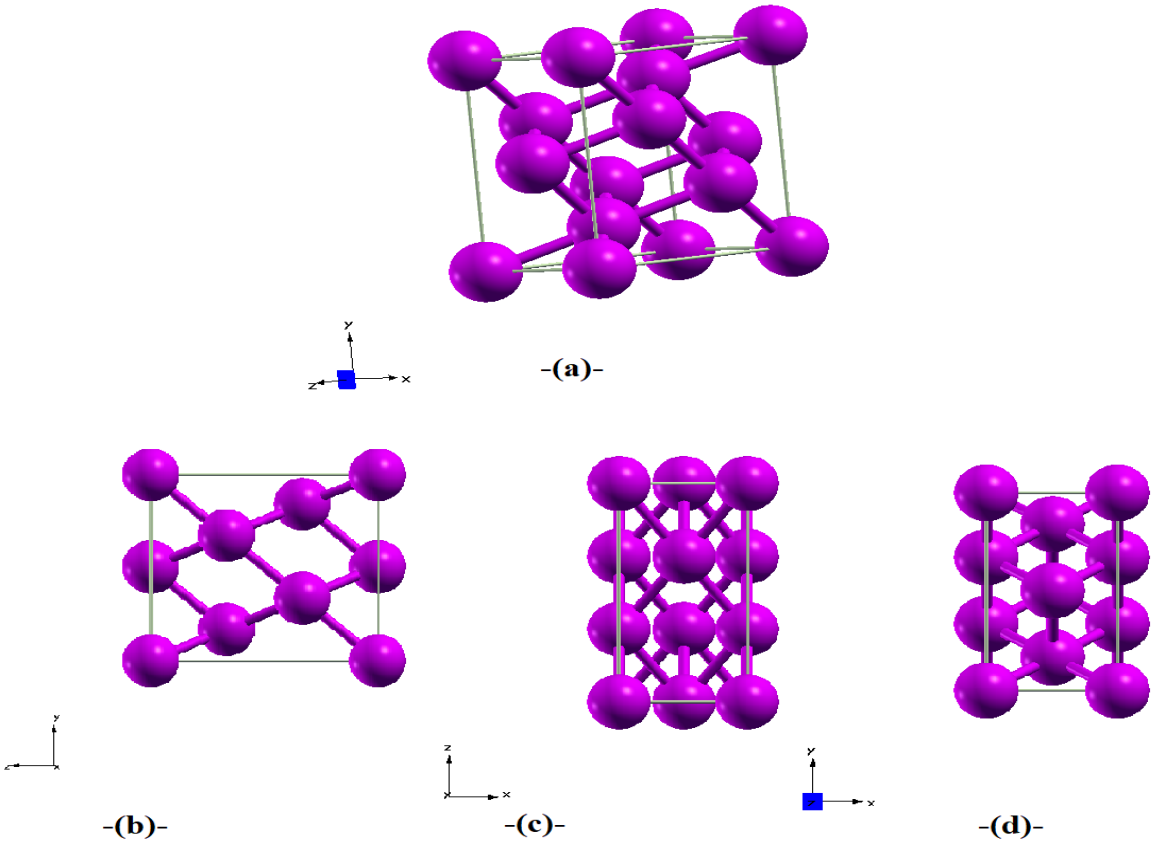

Fig I.9: (a). The fcc crystal structure of Aluminum direction with <111>. **(b).** Aluminum in direction x. **(c).**Aluminum in direction y. **(d).** A1uminum in direction z.

Aluminum "Al"	
Crystal System	face cantered cubic
Space group	m3m
Unit cell	$a_{Al<100>}$= 4.05 Å α = β = ɤ=90°
Unit cell	$a_{Al<111>}$= 2.86Å; $b_{Al<111>}$= 4.96Å; $c_{Al<111>}$=7.01Å α = β = ɤ=90°
Z	13

Table I.7: Crystal structural properties of Al [32].

V.2. Proprieties physiques of Aluminum:

Aluminum used in the majority with a form of alloys, the main constituent of which is aluminum, the additional elements being able to represent up to 15% of its weight. The strength of the aluminum alloy is adapted to the required application.

Aluminum is an excellent conductor of heat and electricity, with the thermal conductivity is used in many applications of heat dissipation, i.e. cooling (such as air conditioning systems in vehicles). And for the same weight, aluminum offers an electrical conductivity twice that of copper, which explains its privileged use in applications of high voltage electricity over long distances [32].

Aluminum Al	
Atomic mass	26.9815386 g
Maximum number of oxidation	3^+
Minimum oxidation number	0
Density at 20 ° C	2.7 g/cm3
Melting point	659.7–660.1 ° C
Volumic mass	2.7kg/dm3
Boiling point	2400–2450 ° C
Thermal conductivity at 20 ° C	272 W / m.K
Rayon de Van der Waals	0.143 nm
Ion beam	0.05 nm
Number of common isotopes	1

Table I.8: Physical properties of Al [35]**.**

VI. Conclusion:

One of our most important conclusions about this chapter is that the copper oxides are transition-metal p-type semiconductors in general and high-TC superconductors in particular. Aluminum is the most abundant metallic element on Earth. It is a light, odorless, tasteless, nontoxic, non-magnetic material and has a high electrical conductivity. In the pure metallic state it oxidizes readily in air to form a stable oxide surface that resists further corrosion. Because of these properties aluminum and its alloys are used extensively in modern industry, technology and everyday life.

In our work, we chose Cu_2O because its center-faced cube structure is close to the aluminum structure, allowing for acceleration in calculation.

References:

[1] P A Korzhavyi and B Johansson,"Literature review on the properties of cuprous oxide Cu_2O and the process of copper oxidation", Technical Report, October 2011, 1404-0344.

[2] Hannes Raebiger, Stephan Lany, and Alex Zunger," Origins of the p-type nature and cation deficiency in Cu_2O and related materials", PHYSICAL REVIEW B 76, 045209, 2007.

[3] D.D. Arhin, Thèse de doctorat, Université de Trento, Italie, 2006.

[4] Mizuno K, Izaki M, et al "Structural and electrical characterizations of electrodeposited p-type semiconductor Cu2O films",J Electrochem Soc 2005;152:C179e82.

[5] Yao LZ, Wang WZ, Wang LJ, Liang YJ, Fu JL, Shi HL. "Chemical bath deposition synthesis of TiO_2/Cu_2O core/shell nanowire arrays with enhanced photoelectrochemical water splitting for H-2 evolution and photostability", Int J Hydrogen Energy 2018,43:15907e17

[6] Kaur, M. Muthe, et al " Growth and branching of CuO nanowires by thermal oxidation of copper". Journal of Crystal Growth, 289(2), 670–675,J. V. (2006).

[7] L. Zhang, J. Li, Z. Chen, Y.Tang, Y. Yu," Preparation of Fenton reagent with H_2O_2 generated by solar light-illuminated nano-Cu_2O/MWNTs composites", 17 January 2006, Pages 292-297.

[8] S. Ghosh, D.K Avasthi, P. Shah, V. Ganesan, A. Gupta, D. Sarangi, R. Bhattacharya, W. Assmann, "Deposition of thin films of different oxides of copper by RF reactive sputtering and their characterization",June 2000, Pages 377-385.

[9] X.M. Liu and Y.C. Zhou, "Electrochemical deposition and characterization of Cu_2O nanowires"Applied Physics A volume 81, pages685–689(2005).

[10] M.F. Al-Kuhaili, "Characterization of copper oxide thin films deposited by the thermal evaporation of cuprous oxide (Cu_2O) "Vacuum, volume 82, issue 6, 19 February 2008, Pages 623–629.

[11] Ako M. Qadir, Ibrahim Y. Erdogan a,b," Structural properties and enhanced photoelectrochemical performance of ZnO films decorated with Cu_2O nanocubes" , Hydrogen Energy, volume 44, issue 34, 12 July 2019, Pages 18694-18702.

[12] J. Li, J.W. Mayer, "Oxidation and protection in copper and copper alloy thin films", J. Appl. Phys., 70 5 (1991) 2820-2827.

[13] Gong, Y. S., Lee, C., & Yang, C. K. (1995). "Atomic force microscopy and Raman spectroscopy studies on the oxidation of Cu thin films". Journal of Applied Physics, 77(10), 5422–5425.

[14] J. Rocchi, "Couplage entre modélisations et expérimentations pour étudier le rôle de l'oxydation et des sollicitations mécaniques sur la rhéologie et les débits de troisième corps solide : cas de l'usure de contacts de géométrie conforme", Thèse doctorat, INSA Lyon (2005).

[15] H.E. Swanson, R.K. Fuyat, "Standard x-ray diffraction powder patterns", Natl. Bur. Stand. (US), 539 2 (1953) 23 correspondant à la fiche pdf 00-005-0667.

[16] Chia-Ying Chiang, Kosi Aroh, Sheryl H. Ehrman," Copper oxide nanoparticle made by flame spray pyrolysis for photoelectrochemical water splitting e Part I. CuO nanoparticle preparation ", International Journal of Hydrogen Energy, 37(6), 4871–4879.

[17] Gassim yamina,"l'influence de la concentration de l aluminium sur les propriétés des couches minces de CuO élaborées par spray pneumatique", mémoire master, université Med khider biskra,2017-2018.

[18] Mr. Kirdous Arezki- Mr. Bouchekhchoukh Athmane ,"Élaboration et caractérisation des couches minces d'oxyde de cuivre : application electrocatalytique sur l'acide ascorbique", mémoire de master, Université A. MIRA - Bejaïa, 02/07/2012.

[19] M.Z. Sahda na- et al , "Fabrication and characterization of crystalline cupric oxide (CuO) films by simple immersion method", Procedia Manufacturing ,2 (2015),379 – 384.

[20] Bacha Rabie , "La synthèse des nano particules de CuO avec la méthode de précipitation sol_ gel, en utilisant le précurseur CuCl2 et l'étude de leurs propriétés structurales et optique" , mémoire master, Université mentouri Constantine-1- , 29 / 04 / 2015.

[21] M.-H.Chang, H.-S.Liu and C.Y. Tai, "Preparation of copper oxide nanoparticles and its application in nanofluid", Powder Technol , 207- 378, (2011).

[22] Fatima Zahra CHAFI,"Deposition of undoped and doped Copper Oxide thin films by Spray Pyrolysis technique: Experiment and Theory", thése de doctora, Université Mohammed V, Rabat, 29 December 2017.

[23] Derkaoui sara, "optimisation de la température du substrat des couches minces de CuO élaborées par spray pneumatique",mémoire master, université Med khider biskra,2017-2018.

[24] Z.Y. Li, Y.C. Zhai, M. Pang, “Effect of particle size on oxidation reaction kinetics parameter of Cu2Opowders”, Adv. Mater., 284 286 (2011) 726-729.

[25] G.T. Tunnel, E. Posnjak, C.J. Ksanda, “Crystal structure of tenorite”, J. Washington Acad. Sci. 23(1933) 195-198.

[26] M. O'KrnrrEl and J.-O. BovlN," The crystal structure of paramelaconite, CunOs", American Mineralogist, Volume 63, pages 180-185, 1978.

[27] Dhanya S Murali and A Subrahmanyam," Synthesis of low resistive p type Cu_4O_3 thin films by DC reactive magnetron sputtering and conversion of Cu_4O_3 into CuO by laser irradiation", Journal of Physics D: Applied Physics, 49 (2016) 375102 (7pp).

[28] Wang Y et al , "Tuning the structure and preferred orientation in reactively sputtered copper oxide thin films",2015 Appl. Surf. Sci. 335 85.

[29] Meyer B K et al, "Binary copper oxide semiconductors: From materials towards devices", Phys. Status Solidi B, 1–23 (2012).

[30] Debbichi, L., Marco de Lucas et al,"Vibrational Properties of CuO and Cu_4O_3 from First-Principles Calculations, and Raman and Infrared Spectroscopy", The Journal of Physical Chemistry C, 116(18), 10232–10237 ,2012.

[31] D. Djurek a,n et al, "Magnetic properties of nanoscaled paramelaconite Cu4O3x (x¼0.0 and 0.5) ", Journal of Magnetism and Magnetic Materials, 3 April 2014.

[32] M.H Jacobs, "Introduction to Aluminum as an Engineering Material", TALAT Lecture 1201, 1999, EAA - European Aluminum Association.

[33] NAOUI Hadjer, "Effet du double traitement sur le comportement à la corrosion de l’alliage 6060", mémoire master, Université de M’sila, 2015 / 2016.

[34] Nakashima, Philip N.H., "The Crystallography of Aluminum and Its Alloys" in Encyclopedia of Aluminum and Its Alloys ed. George E. Totten, Murat Tiryakioğlu and Olaf Kessler (Boca Raton: CRC Press,16 Nov 2018), 488 – 586.

[35] Yakoubi Myliada," Effet des petites déformations par compression Surle comportement à la corrosion de l’alliage d’aluminium de fonderie Al4⁒Cu", Université Mouloud Mammeri, Tizi-ouzou,2015.

Chapter II:

Density Functional Theory (DFT)

I. Introduction :

The following chapter allows to lay the theoretical foundations of the calculations carried out during this work. Understanding the different properties of materials involves studying the system of electrons and strongly interacting nuclei that constitute it. The interactions between a large number of electrons give a rise to the properties of solids. The calculation of the electronic structure of molecules and solids is a discipline that arose during the last century. It has grown tremendously over of the last years thanks to advances in computing and the increasing of computing power in computers . For the calculation of electronic, structural and mechanical properties...etc of the most complex systems using the ab-initio methods which have now become a basic tool [1].

Ab-initio modeling is based on the first principles of quantum physics, as determined (in our case) by the Schrödinger equation. The objective is to solve this equation in systems containing a large number of electrons, cases for which there is no analytical solution, so various approximations have to be used. One of the most used methods is the density functional theory (DFT).

II. Schrödinger's equation:

The Schrödinger equation is a partial differential equation that describes the quantum state change of a physical system that can be considered a single system consisting of light particles (electrons) and heavy (cores) in their stationary state, this equation was formulated by physicist Erwin Schrödinger in 1925 and published in 1926, where is occupies a special importance in quantum mechanics and is the primary relationship to the dynamics of classical mechanics [2]. Formulated as follows:

$$\hat{H}\Psi\ (R_I, r_i) = \hat{E}\Psi\ (R_I, r_i) \qquad \text{(II.1)}$$

$\Psi(R_I, r_i)$: Represents the total wave function of the system, r_i and R_I: Spatial coordinates of the electrons and nuclei respectively, $\hat{E}$: total energy of the system.

$$\Psi(R_I, r_i) = \Psi_n(\overrightarrow{R_1} \dots \overrightarrow{R_N})\Psi_e\ (\overrightarrow{r_1} \dots \overrightarrow{r_n}) \qquad \text{(II.2)}$$

$\hat{H}$: Being the total Hamiltonian of the quantum system studied. In the non-relativistic case it is written in the form:

$$\hat{H}_T = \hat{T}_n + \hat{T}_e + \hat{V}_{n-e} + \hat{V}_{n-n} + \hat{V}_{e-e} \qquad \text{(II.3)}$$

$\hat{T}_n = \frac{-\hbar^2}{2m_n}\sum_I \nabla_j^2$: Represent the kinetic energy of nuclei.

$\hat{T}_e = \frac{-\hbar^2}{2m_e}\sum_i \nabla_i^2$: Represent the kinetic energy of electrons.

$\hat{V}_{n-n} = \frac{1}{2}\sum_{I<J} \frac{e^2 Z_I Z_J}{|\vec{R_I} - \vec{R_J}|}$ **:** The potential energy of interaction between the nuclei.

$\hat{V}_{e-n} = -\sum_{I\neq i} \frac{e^2 Z_I}{|\vec{ri} - \vec{R_I}|}$ **:** The potential energy of electron-nucleus attraction.

$\hat{V}_{e-e} = \frac{1}{2}\sum_{i<j} \frac{e^2}{|\vec{R_I} - \vec{R_J}|}$ **:** The potential energy of repulsion between electrons.

This equation becomes as follows:

$$\hat{H}_T = \frac{-\hbar^2}{2}\left(\sum_I \frac{\nabla_I^2}{m_I} + \sum_i \frac{\nabla_i^2}{m_e}\right) + \frac{1}{2}\sum_{I<J} \frac{e^2 Z_I Z_J}{|\vec{R_I} - \vec{R_J}|} - \sum_{I\neq i} \frac{e^2 Z_I}{|\vec{ri} - \vec{R_I}|} + \frac{1}{2}\sum_{i<j} \frac{e^2}{|\vec{R_I} - \vec{R_J}|} \quad \text{(II.4)}$$

The observable physical properties are all contained in this last equation (II.4). However due to its complexity (equation with N + M particles) it is impossible to solve it directly, it is therefore resorted to many approximations presented below [3].

III. Born-Oppenheimer approximation:

As we know, the terminology of molecular spectra consists of parts of different sizes, the greatest contribution comes from the electronic movement around the nuclei, followed by a contribution from nuclear vibrations, and finally from the parts generated by nuclear cycles. It is clear that the reason for the existence of such an arrangement is the size of the mass of the nuclei in relation to the electrons [4].

Scientists Max Born and Robert Oppenheimer developed the first approximation we could make [4] in 1927, they simplified equation (II.1) and suggested that the movement of nuclei can be separated from the movement of electrons, which is justified by the fact that the mass of the nucleus is much greater than the mass of electrons. Thus, the speed of movement of the electron is much higher than the speed of the nucleus (the nucleus is not mobile relative to the electrons) [1, 5].

By adopting this hypothesis, we simplify the Schrödingerrop equation, especially Hamilton, where the kinetic energy of the nucleus becomes zero $\hat{T}_n = 0$ and the reaction energy of the

nucleus $\hat{V}_{n-n}$ =0 becomes constant (the spatial derivatives of the nucleus is zero), and we have a new Hamiltonian in the equation as follows:

$$\hat{H}_T = \hat{T}_e + \hat{V}_{n-e} + \hat{V}_{e-e} \quad \text{(II.5)}$$

$$\hat{H}_{B\text{-}O} = \frac{-\hbar^2}{2}\sum_i \frac{\nabla_i^2}{m_e} - \sum_{I\neq i} \frac{e^2 Z_I}{\left|\vec{ri} - \vec{R_I}\right|} + \frac{1}{2}\sum_{i<j} \frac{e^2}{\left|\vec{R_I} - \vec{R_J}\right|} \quad \text{(II.6)}$$

$$\hat{H}_{B\text{-}O}\Psi_e(R_I, r_i) = \hat{E}_e\Psi_e(R_I, r_i) \quad \text{(II.7)}$$

$$\left[\frac{-\hbar^2}{2}\sum_i \frac{\nabla_i^2}{m_e} - \sum_{I\neq i} \frac{e^2 Z_I}{\left|\vec{ri} - \vec{R_I}\right|} + \frac{1}{2}\sum_{i<j} \frac{e^2}{\left|\vec{R_I} - \vec{R_J}\right|}\right] \Psi_e(R_I, r_i) = \hat{E}_e\Psi_e(R_I, r_i) \quad \text{(II.8)}$$

Ψ_e : Is the electronic wave function describing the movement of electrons in the field of nuclei.

$$\hat{E}_e = \hat{E}_e(R_I) = \hat{T}_e + \hat{E}_{e\text{-}e} + \hat{E}_{e\text{-}n} \quad \text{(II.9)}$$

$\hat{E}_e$: It represents the electronic energy where the contributions of the kinetic energy T_e. And potential energies are collected due to the interaction between the $E_{e\text{-}e}$ electrons and those resulting from the interaction of the $E_{e\text{-}n}$ electronic nucleus [6].

All Hamilton terms related to the nuclei are eliminated. However, this approximation alone is not sufficient to solve the Schrödinger equation, due to the complexity of the electron and electron interactions. So we resort to almost another.

IV. Approximation Hartree:

This approximation [7] is called the free electron approximation. We consider the electrons to be independent, because each electron moves in an intermediate field created by the nucleus and other electrons, and to each electron corresponds an orbital. The total wave function is written as a mono-electronic wave function product [8], so that:

$$\Psi(\vec{r_1}\ldots\vec{r_n}) = \prod_i^n \varphi_i(\vec{r_i}) \quad \text{(II.10)}$$

In this approximation, the global Hamiltonian is written as a sum of the monoelectronic Hamiltonians. And Schrodinger's equation to an electron is written in the form [5]:

$$\left[-\frac{1}{2}\nabla^2 + U_i(\vec{r}) + V_i(\vec{r})\right]\varphi_i(\vec{r}) = \varepsilon_i\varphi_i(\vec{r}) \quad \text{(II.11)}$$

$\varphi_i(\vec{r})$: It is the effective electronic mono equation.

$U_i(\vec{r}) = \sum I \frac{2Z}{|\vec{r}-\vec{R_I}|}$ **:** It's the potentials that produced by all nuclei.

$V_i(\overrightarrow{r}) = \int d^3\overrightarrow{r'} \frac{2\rho(\overrightarrow{r'})}{|\vec{r}-\vec{r'}|}$ **:** Is the average potential produced by the other electrons, called Hartree potential.

$\rho(\overrightarrow{r'}) = \sum_{j=1;j\neq i}^{N} |\varphi_i(\vec{r})|^2$ **:** Represents the electron density.

$$E = \sum \varepsilon_i - E_V + E_U \qquad (II.12)$$

E**:** Is total system energy **(**the sum of the ε_i relates to the N lower energy states, E_U is the potential energy of nucleus-nucleus interaction, E_V is energy of Hartree :

$$(E_v = \frac{1}{2} \int \frac{\rho(\overrightarrow{r_j})\rho(\overrightarrow{r})}{|\vec{r}-\overrightarrow{r_j}|} d^3\vec{r} d^3\overrightarrow{r'_j})).$$

This approximation is based on the free electron hypothesis, which amounts to ignoring the interactions between electrons and spin states [6]. This has two important consequences:

- First is the Pauli Exclusion Principle, which states that no two spin-orbitals in an atom can be the same. This allows an orbital to occur twice, but only with opposite spins [9].
- Second, the metaphysical perspective of the quantum theory implies that individual interacting electrons must be regarded as indistinguishable particles. One cannot uniquely label a specific particle with an ordinal number, the indices given must be interchangeable. Thus each of the N electrons must be equally associated with each of the N spin-orbital's [9].

To solve the electronic mono equation, it is necessary to know the shape (V_i) which in turn requires knowledge of density ($\rho(\overrightarrow{r'})$), but there is no direct method that allows finding the solution simultaneously [5].

We conclude that the solution offered by Hartree approximation is not completely compatible with reality. The result is that the electrons represent identical, indistinguishable particles and obey the Pauli Exclusion Principle [10]. Therefore, the overall wave function of the electronic system must be asymmetric by contributing to the exchange of two electrons [5]. And the problem also lies in finding the best spin orbits which give the lowest possible system power, according to the shifting principle, this goal is achieved using a consistent Hartree-Fock method [11].

The main flaw in Hartree's equation is that it ignores the Pauli principle. If we bring in the Pauli principle, we end up with the Hartree-Fock equation.

V. The approximation Hartree-fock:

In this new approximation known as the Hartree-Fock approximation, generalized the concept by showing that the Pauli exclusion principle (which requires two electrons not to be able to occupy the same spin – orbital) is taken into account, and proposed to write the total wave function of the electronic system not as a direct product of the mono-electronic wave functions, but as a Slater determinant [5]:

$$\Psi\left(\vec{r}_1\vec{\eta}_1 \ldots . \vec{r}_n\vec{\eta}_n\right) = \frac{1}{\sqrt{N!}}\begin{vmatrix} \varphi_1(\vec{r}_1\vec{\eta}_1) & \varphi_1(\vec{r}_2\vec{\eta}_2) & \ldots & \varphi_1(\vec{r}_n\vec{\eta}_n) \\ \varphi_2(\vec{r}_1\vec{\eta}_1) & \varphi_2(\vec{r}_2\vec{\eta}_2) & \ldots & \varphi_2(\vec{r}_n\vec{\eta}_n) \\ \vdots & \vdots & & \vdots \\ \varphi_n(\vec{r}_1\vec{\eta}_1) & \varphi_n(\vec{r}_2\vec{\eta}_2) & \ldots & \varphi_n(\vec{r}_n\vec{\eta}_n) \end{vmatrix} \quad \text{(II.13)}$$

Where $\vec{r}$ and $\vec{\eta}$ are the space and spin variables respectively.

With $\frac{1}{\sqrt{N!}}$ The normalization factor, N: being the number of electrons.

We see that the determinantal form of the wave function respects the Pauli principle.

The effective electron energy can be found using the variation method. In this method, the best wave function is sought by minimizing the effective electron energy relative to the parameters of the wave function. Using this idea, Fock and Slater simultaneously and independently developed what are now well known as the Hartree-Fock equations [12].

If we limit ourselves to closed-shell systems, that is to say without single electrons, the Hartree-Fock system of equations will be simplified in the following form, which only takes into account the space orbitals[12].

$$\mathrm{F_i}(1)\,\varphi_i(1) = \varepsilon_i\varphi_i(1)$$

ε_i: is the energy of the orbital i.

$\mathrm{F_i}$: is the Fock operator given by:

$$\mathrm{F_i} = \mathrm{h}(1) + \sum\left[2J_j(1) - K_j(1)\right] \quad \text{(II.14)}$$

The term h (1) is the operator for an electron h (1) = $-\frac{1}{2}\nabla_1^2 - \sum_{A=1}^{N}\frac{Z_A}{r_{1A}}$ **.** This term takes into account the movement of the electron and the interactions of the electron nucleus [12].

The term $J_j(1)$ is the coulomb operator to which the coulomb integral corresponds.

$$J_j(1) = \int \varphi_j^*(2) \frac{1}{r_{12}} \varphi_j(2) dr_2 \quad \text{(II.15)}$$

$K_j(1)$ This is the exchange operator to which corresponds the following exchange integral:

$$K_j(1)\varphi_k(1) = \left[\int \varphi_j^*(2) \frac{1}{r_{12}} \varphi_k(2) dr_2\right] \varphi_j(1) \quad \text{(II.16)}$$

Coulomb and exchange integrals describe interactions between electrons [12].

The Hartree-Fock equation is written as in the following form [13]:

$$\left[-\frac{1}{2}\nabla^2 + U_i(\vec{r}) + V_i(\overrightarrow{r}) + V_x(\overrightarrow{r})\right] \varphi_i(\vec{r}) = \varepsilon_i \varphi_i(\vec{r}) \quad \text{(II.17)}$$

Where $V_x(\overrightarrow{r})$ is the nonlinear and nonlocal exchange potential introduced by Fock, it is defined by its action on a wave function $\varphi_i(\vec{r})$ [13]:

$$V_x(\overrightarrow{r}) = -\int \frac{\sum \varphi_i^*(\overrightarrow{r'}) \varphi_i(\vec{r}) \varphi_j^*(\overrightarrow{r'}) \varphi_j(\vec{r})}{|\vec{r} - \vec{r}_i|} d^3\vec{r}_i \quad \text{(II.18)}$$

Using the variational method, we can calculate the energy of the system of "n" electrons E^{HF} (Hartree-Fock energy):

$$E^{HF} = \frac{\langle \Psi | H | \Psi \rangle}{\langle \Psi | \Psi \rangle} \quad \text{(II.19)}$$

$\langle \Psi | \Psi \rangle = 1$ Because ψ is normalized, and therefore we obtain E^{HF} as a sequence:

$$E^{HF} = \langle \Psi | H | \Psi \rangle \quad \text{(II.20)}$$

$$E^{HF} = \left\langle \Psi \left| -\frac{1}{2}\nabla^2 \right| \Psi \right\rangle + \langle \Psi | U_i(\vec{r}) | \Psi \rangle + \left\langle \Psi \left| V_i(\overrightarrow{r}) \right| \Psi \right\rangle + \left\langle \Psi \left| V_x(\overrightarrow{r}) \right| \Psi \right\rangle \quad \text{(II.21)}$$

Hartree-Fock energy becomes the sum of the kinetic energy of the electrons, external energy, Hartree energy, and exchange energy[13]:

$$E^{HF} = E_{cin} + E_{ext} + E_H + E_X = 2\sum_{i=1}^{n} h_{ii} + \sum_{i,j}^{n} (2J_{ij} - K_{ij}) \quad \text{(II.22)}$$

The difference between the exact nonrelativistic energy and the Hartree-Fock energy in a full basis is called the correlation energy E_{corr}, it is a measure of the error introduced by the Hartree-Fock approximation and it is mainly due to the almost instantaneous repulsion of electrons which does not take into account the Hartree potential $V_i(\overrightarrow{r})$[13].

$$E_{corr} = E_{exact} - E^{HF} \quad \text{(II.23)}$$

The Slater determinant therefore makes it possible to obtain an antisymmetric multielectronic wave function respecting the Pauli rule. But, despite the very satisfactory results obtained, this approach neglects the term of electronic correlation of the system [13].

Several methods have been developed to go beyond the Hartree-Fock method and take into account electronic correlations, these are the methods based on the density functional theory [14] which consist in describing the system in function of its mono-electronic density [13].

VI.The Thomas-Fermi approximation (The beginnings of the DFT):

The fundamental concept of DFT is that the energy of an electronic system can be expressed in terms of its density. This is in fact an old idea dating mainly from the work of Thomas [15] and Fermi [16]. The use of electron density as a fundamental variable to describe the properties of the system has always existed as a leitmotiv since the first approaches to the electronic structure of matter but has only been proven by the proof of the two theorems of Kohn and Sham [17].

Shortly after formulating the laws of quantum mechanics, Thomas and Fermi (1927) actually attempted to express the total energy as a function of density, They used the local expression for the kinetic energy, the exchange energy and the bonding of the homogeneous electron gas to construct the same quantities for the heterogeneous system [13]. The Thomas-Fermi energy as a function of density is:

$$E_{T-F}[\rho] = T_{T-F}(\rho) + E_{ext}(\rho) + E_H(\rho) \tag{II.24}$$

$$E_{T-F}[\rho] = \frac{3}{10}(3\pi^2)^{\frac{2}{3}} \int \rho^{\frac{5}{3}}(r) d^3r + \int V_{ext}(r)\, \rho(r) dr + \frac{1}{2} \int \frac{\rho(r)\rho(r')}{|r-r'|} dr dr' \tag{II.25}$$

The Thomas and Fermi approximation is a local density approximation that ignores the correlation of electrons, because it considers an inhomogeneous gas to be locally homogeneous. Improvements have been made to this model by adding other effects such as [18].

The exchange effect introduced by Dirac which results in the addition of an additional term in the Thomas-Fermi energy (Thomas-Fermi-Dirac model) [18].

$$E_{TDF} = E_{TF}(\rho) - C_x \int \rho^{\frac{4}{3}}(\vec{r}) d^3r \tag{II.26}$$

The correlation effect proposed by Wigner [18]:

$$E_C(\rho) = -a \int \frac{\rho^{\frac{4}{3}}(\vec{r})}{b+\rho^{\frac{1}{3}}(\vec{r})} d^3r \quad \text{(II.27)}$$

Despite these improvements, this model is still inadequate.

VII. Density Functional Theory (DFT):

DFT is a quantum computation method used by researchers in the context of numerical simulations in physics and chemistry, it makes it possible to reproduce the electronic structure of complex systems in general faithfully and in a fairly short period of time thanks to the development of computers, it is considered "ab-initio method" because it uses strict theories ("Hohenberg-Kohn", Kohn-Sham "...), so the results are not dependent on a modifiable parameter by the user. However, the term interchange and correlation makes any an accurate solution is impossible. As in the case of quasi-experimental methods, it is necessary to approximate this function, this classifies it as a separate method (between quasi-experimental and ab-initio) between methods of numerical computation. We start by evoking the history of the development of this method. From the Schrödinger equation To the Cohn-Sham equations.

Density functional theory (DFT) is the most widely used method for studying molecular systems of large size, it has been largely successful in describing structural and electronic properties in a large class of materials ranging from atoms and molecules to simple crystals and more complex molecular systems, and has been extensively researched from a global perspective.

The birth of the modern functional density theory (DFT) came with the publication of two articles by Hohenberg and Kuhn in 1964 [19], and Kohn and Scham in 1965 [20], which laid the foundations for this theory. The goal of DFT is to determine, using knowledge of only the electron density ρ(r) r, the ground-state properties of a system consisting of a fixed number of electrons, interacting with point nuclei. DFT constitutes an accurate theory of electronic correlation effects.

VII.1. Hohenberg and Kohn theorems:

The foundational principle of DFT can be summarized in two theories, first introduced by Hohenberg and Kohn [17], and the latter aiming to make DFT an accurate theory of multi-body

systems. This formula applies to any system of particles interacting with each other with an external voltage $V_{eff}(r)$.

Hohenberg and kohn's theories formulated in 1964 [19] made it possible to give a Consistency with models developed on the basis of the theory eventually proposed by Thomas and Fermi From the thirties. The two theories lie in:

a. Theorem 1:

"The total energy of the ground state E is a unique functional of the particle density ρ (r) for a given external potential V_{ext} (r)".

The consequence of this fundamental theorem of DFT is that the variation of the external potential then implies a variation of the density:

$$E[\rho(r)] = F[\rho(r)] + V_{ne}[\rho(r)] \quad \text{(II.28)}$$

$$E[\rho(r)] = F[\rho(r)] + \int \rho(r) V_{ext}(r) d^3r \quad \text{(II.29)}$$

$$F[\rho(r)] = T[\rho(r)] + \frac{1}{2} \int \int \frac{\rho(r)\rho(r')}{|r-r'|} d^3r d^3r' + E_{xc}[\rho(r)] \quad \text{(II.30)}$$

F[ρ (r)]: Is a universal functional of hohenberg and kohn and groups together all the terms independent of the external potential.

$V_{ne}[\rho(r)]$: Nucleus-electron potential energy.

$T[\rho(r)]$: The potential energy of repulsive electron-electron interaction.

$E_{xc}[\rho(r)]$: The exchange-correlation energy.

The first theorem [21] consists in giving a theoretical justification to the idea that at a given electron density correspond a single external potential.

b. Theorem 2:

"The total energy functional of any multi-system particles has a minimum which corresponds to the ground state and the density of ground state particles".

The energy of the ground state of an electronic system in an external potential is determined by the variation method [23].

$$E_0 = E(\rho_0) = min\, E(\rho) \quad \text{(II.31)}$$

To find $\rho_0(\vec{r})$ corresponding to the ground state, we must minimize E(ρ), with the condition $\int \rho(\vec{r})\, d^3r = N$:

$$\frac{\delta}{\delta\rho}\left\{ E(\rho) - \lambda \int \rho(r)\, d^3r \right\} = 0 \qquad \text{(II.32)}$$

Unfortunately in this theorem the functional $F[\rho(r)]$ is difficult to approach directly to obtain quantitative results. It is thanks to a simple but ingenious idea of Khon and Sham who found a solution to this term $E(\rho)$.

VII.2. Kohn and Sham's equations:

Kohn-Sham has developed a method which consists in paralleling the equation (II.23) with the equation governing a system of electrons without interaction in an external potential $V_{eff}(r)$ [22]:

$$\frac{\delta E[\rho]}{\delta\rho} = \frac{\delta T_0}{\delta\rho} + V_{eff}(r) = \mu \qquad \text{(II.33)}$$

With the effective potential $V_{eff}(r)$:

$$V_{eff}(r) = V_{ext}(r) + \int \frac{\rho(r')dr'}{|r-r'|} + \frac{\delta E_{xc}[\rho]}{\delta\rho(\rho)} = V_{ext}(r) + H_{hartree}(\rho) + V_{xc}(r) \qquad \text{(II.33)}$$

Where $V_{xc}(r)$ is the exchange-correlation potential, functional derivative of $E_{xc}[\rho]$. The previous equation is exactly the same as that of Hohenberg and Kohn's theory for a system of non-interacting electrons moving in an effective potential of the form of $V_{eff}(r)$[22].

By applying the variational principle, we then obtain a set of equations of the Hartree Fock type which we solve by an iterative process:

$$\left[-\frac{1}{2}\nabla^2 + V_{eff}(r)\right]\varphi_i(r) = \varepsilon_i\varphi_i(r) \qquad \text{(II.34)}$$

The electron density is then obtained by the summation:

$$\rho(r) = \sum|\varphi_i(\vec{r},\vec{\eta})|^2 \qquad \text{(II.35)}$$

We choose a test density from which we calculate an effective potential $V_{eff}(r)$. By injecting $V_{eff}(r)$ into expression (II.34) we obtain a new electron density (II.35). Convergence is then reached when the effective potential no longer varies.

The Hartree-Fock and Kohn-Sham quantum theories both lead to a system of mono-electronic equations to be solved, but the Kohn-Sham formalism nevertheless allows part of the

correlation to be taken into account, intrinsically. electronic(which the Hartree-Fock method does not)[22].

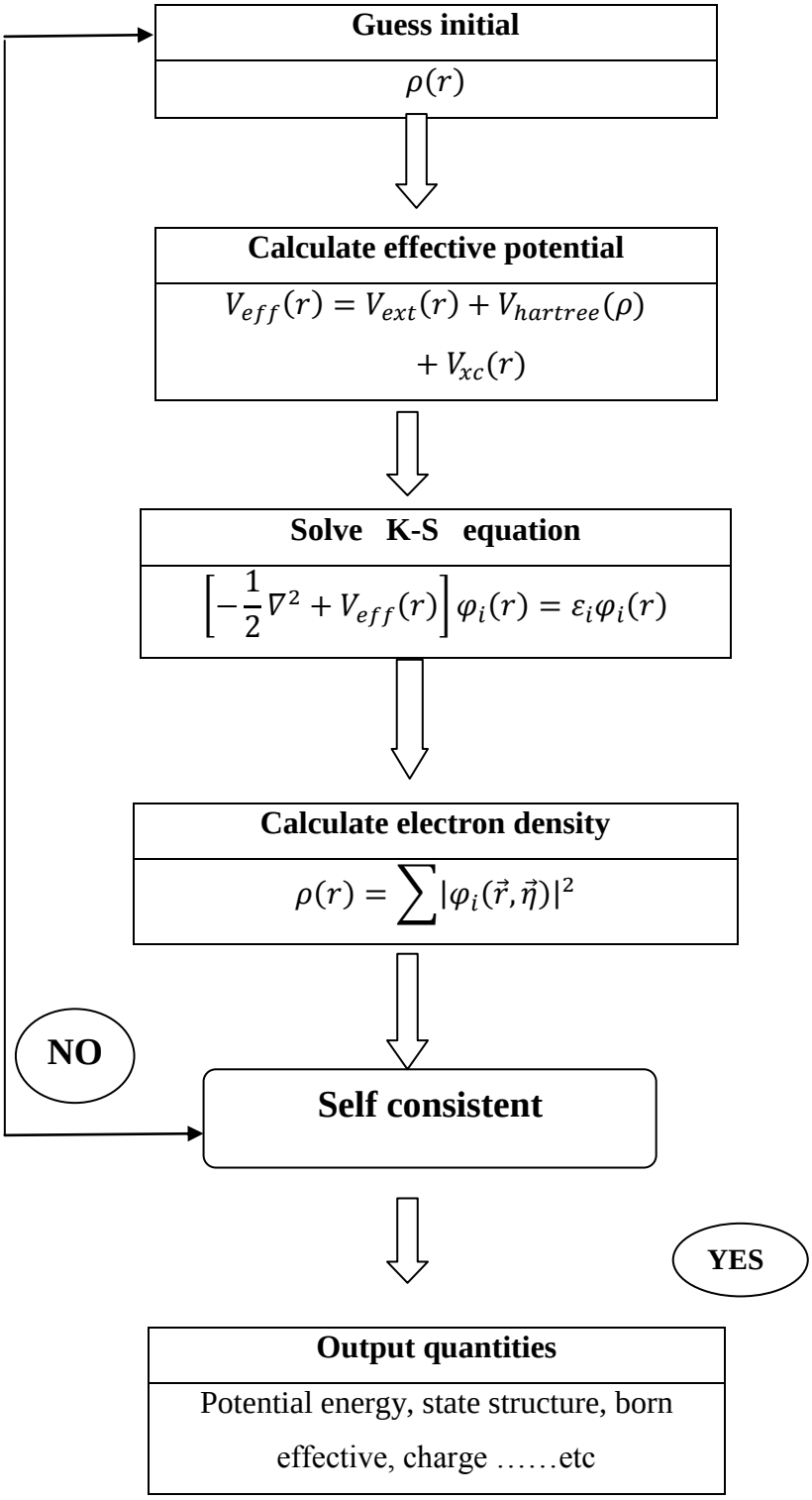

Fig II.1: Flowchart representing the principle of solving Kohn-Sham's equations by diagonalization of the Hamiltonian matrix.

This resolution is done in an iterative manner using a self-consistent cycle of iterations, we summarize this cycle by the following steps [3] (See figure II.1):

1. Start with a test density for the first iteration.

2. Calculate the density and correlation exchange potential for a point.

3. Solve the Kohn-Sham equation.

4. Calculate the new density.

5. Check the convergence criterion (by comparing the old and the new density).

6. Calculate the different physical quantities (Energy, forces,…), and of calculation.

VII.3. The exchange-correlation approximations:

The main problem with DFT is that the exact functionals for exchange and correlation are not known except for free electron gas. However, Approximations exist and allow the calculation of certain physical quantities.

a. Local density approximation LDA :

The local density approximation (LDA or LSDA) is based on the assumption that the exchange and correlation term depends only on the local value of the electronic density ρ (r). It is then expressed in the following way:

$$E_{xc}^{LDA} = \int \rho(r)\varepsilon_{xc}\ [\rho\ (r)]dr \qquad \text{(II.36)}$$

Where ε_{xc} is the energy of exchange and correlation.

Using the LDA we implicitly assume that one can obtain the exchange-correlation energy for an inhomogeneous system by considering the electron gas as homogeneous in infinitesimal portions of it. The LDA method tends to underestimate the exchange term while it overestimates the correlation term, which because of the compensation between these two terms gives a fairly good result in the end. However, it does not describe well the systems where the density varies abruptly.

b. Generalized gradient approximation (GGA):

The GGA considered as the 2nd degree of approximation attempts to correct the defects of the LDA, as this approximation consists in taking into account local variations in the electronic density ρ (r) through its gradient$\nabla\rho\ (r)$. The inhomogeneity of the electronic density is thus taken into account. The term of exchange and correlation is then expressed by equation :

$$E_{xc}^{GGA}[\rho(r)] = \int \rho(r)\varepsilon_{xc}\,[\rho\ (r), \nabla\rho\ (r)]dr \qquad \text{(II.37)}$$

Where $\nabla\rho\ (r)$ is gradient of electronic density.

VIII. Pseudopotential:

Pseudo-potentials are an essential element in solid-state physics calculations due to the great simplification they provide, and is the most important approach to reducing the computational burden due to core electrons [23].

Core electrons are not especially important in defining chemical bonding and other physical characteristics of materials, these properties are dominated by the less tightly bound valence electrons. so it then the simplification of the calculations of electronic structures by elimination of heart states. The strong ionic potential will be replaced with weaker pseudopotential which gives identical valence electron wave functions.

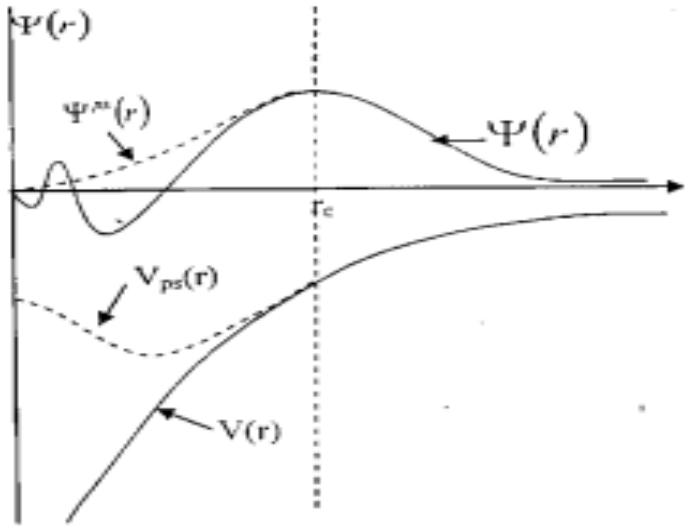

Fig II.2: Illustration schematizes the potential of all-electron (solid lines), pseudo-electron (broken lines) and their corresponding wave functions [24].

Practically, the wave functions Ψ (r) representing the valence electrons are replaced by pseudo-wave functions Ψps (r). The equality Ψps (r) = Ψ (r) is imposed on the outside of a sphere of radius (rc) around the atom and inside this sphere, the shape of Ψps(r) is chosen so as to remove knots and oscillations due to the orthogonality of the wave functions [25].

IX. Sampling of the Brillouin zone:

In the study of solids, it is very often necessary to calculate an average of a periodic function of $\vec{K}$ (wave vector) over the Brillouin zone (ZB). Such calculations are often long and complicated since in principle they require knowledge of the values of the function at any point of ZB and because of the infinite number of electrons, an infinite number of k points are present in this area. In practice, knowledge of the values of functions of a reduced set of points **k** in ZB is sufficient to obtain the mean value of these functions across ZB. To achieve high accuracy in calculations, it is generally necessary to know the values of the function of a sufficiently large set of points. Many procedures exist to generate tilings for Points $\vec{K}$, we can cite that of Chadi and Cohen [26] and that of Monkhorst and Pack [27].

X. Cut off energy:

In principle, the plane wave base is complete but infinite (the number of vectors $\vec{G}$ is infinite). However, the fact that plane waves of weaker kinetic energy play a more important role than those with greater kinetic energy. In practice, we can therefore limit the base used to solve the Kohn and Sham equations, and only take those which have a kinetic energy less than a certain energy called the cut-off energy $E_{cut\text{-}off}$:

$$\frac{\hbar(K+G)^2}{2m_e} < E_{cut} \qquad \text{(II.38)}$$

The cut-off energy depends significantly on the type of chemical element of the system considered and therefore on the corresponding pseudo potentials, It plays an important role in the precision and duration of the calculation, where if it is too low, the number of plane waves in the calculation is not sufficient to represent the wave functions and charge density well, But the computation time increases sharply with the value of E_{cut} we must therefore determine a realistic E_{cut} at the level of the computation time for which the total energy converges with the desired precision [28].

XI. Murnaghan's equation:

Murnaghan's equation of state comes from the assumption of a linear behavior of the bulk modulus of a solid compressed to a finite strain with respect to pressure. For a fixed number of particles at the temperature of absolute zero, the link between pressure P and volume V reads :

$$p(V) = \frac{B_0}{B'_0}\left[\left(\frac{V_0}{V}\right)^{B'_0} - 1\right] \quad \text{(II.39)}$$

V_0 is the lowest-energy atomic volume. B_0 is the so-called bulk modulus and B'_0 its derivative with respect to pressure.

Furthermore, at zero temperature, the pressure may be written as a function of a volume only:

$$\mathrm{p(V)} = \frac{-\mathrm{dE(V)}}{\mathrm{dV}} \quad \text{(II.40)}$$

E(V) [29] Is obtained by a straightforward integration of Equation (II.41)and assuming B_0 and B_0 to be independent of the volume:

$$\mathrm{E(V)} = \mathrm{E_0} + \frac{\mathrm{B_0 V}}{\mathrm{B'_0}}\left[\left(\frac{\mathrm{V_0}}{\mathrm{V}}\right)^{\mathrm{B'_0}} \frac{1}{\mathrm{B'_0 - 1}} + 1\right] - \frac{\mathrm{B_0 V_0}}{\mathrm{B'_0 - 1}} \quad \text{(II.41)}$$

E_0 : the lowest energy per atom.

If the B_0 and B'_0 parameters are supposed to be V-independent, then expression (II.41) is possible solution for the system of Equations (II.39)and (II.40) [30].

XII. QUANTUM ESPRESSO:

Quantum Espresso is an acronym for open-Source Package, which is an integrated suite of computer codes for electronic-structure calculations and materials modeling, based on density-functional theory, plane waves, and pseudo potentials (norm-conserving, ultra soft, and projector-augmented wave) [31]. As its acronym indicates Quantum Espresso is a free research program suite for Research in Electronic Structure, Simulation, and Optimization, and the program is licensed under the GNU GPL, it can also be used, both for metals and for insulators. Self-consistent calculations are done using the PWSCF program and are done iteratively within the program.

XIII. The SIESTA program:

SIESTA (acronym for Spanish Initiative for Electronic Simulations with Thousand of Atoms) [32] is a code (program) developed by Soler et al, in 2002, designates both a method, and its numerical implementation for performing ab-initio electronic structure, and it is used especially for the simulation of molecular dynamics of physical and chemical processes that occur at the atomic scale.

It is based on the theory of the standard density functional with the local density (LDA) or generalized gradient (GGA) approximation, in which it uses pseudopotentials with conserved norms and a base made up of digitized atomic orbitals. However, instead of being developed on a plane wave basis the wave function is developed on an atomic orbital basis.

XIV. Conclusion:

The density functional theory quickly established itself as a relatively fast and reliable way to simulate electronic and structural properties for most of the elements of the periodic table ranging from molecules to crystals.

In this chapter, we have presented the DFT theory and we have discussed mainly the essential points and relating to our work. Nowadays DFT is a powerful tool which shows great success in many applications. Within the framework of the DFT, there are techniques of calculation of the electronic structure developed during the last decades are numerous, and in particular, the ab-initio methods which have become today a basic tool for the calculation. Electronic and structural properties of the most complex systems and also a tool of choice for the prediction of new materials.

Ab-initio studies carried out on all existing materials are numerous, they have given reliable results by comparing them with experimental measurements.

References:

[1] Payne MC, Allan DC, Arias TA, Joannopoulos JD, "Iterative minimization techniques for ab initio total-energy calculations: molecular dynamics and conjugate gradients ", Reviews of Modern Physics, 1992; 64: 1045-1098.

[2] Djemia P, Dugautier C, Chauveau T, Dogheche E, De Barros M.I, Vandenbulcke L, "Mechanical properties of diamond films: a comparative study of polycrystalline and smooth fine-grained diamonds by Brillouin Light Scattering", J. Appl. Phys, vol 90, n° 8 2001, p. 3771-3779.

[3] Ilyes Mesbahi, "Etude DFT des propriétés électroniques de films minces MoSe",Mémoire de master, Université mouloud Mammari, Tizi-ouzou,12/07/2018.

[4] Born M & Oppenheimer R, "Zur Quantentheorie der Molekeln", Ann. Phys, Leipzig 84, 457–484,1927.

[5] Boucheriguene Hayat, "Les propriétés géométriques et magnétiques des agrégats de fer (Fen) en fonction de leur taille (n=1-15) " , mémoire master, Université de Bouira, 2013/2014.

[6] Samira Chelli," Etude des propriétés structurales, électroniques, thermiques et thermodynamiques des alliages ternaires BaxSr1-xS, BaxSr1-xSe et BaxSr1-xTe ", thèse doctorat, Badji mokHtar university Annaba, 2015.

[7] C.Friedrich and A. Schindimayr, "Many body Perturbation Theory: The GW Approximation",John von Neumann Institute for Computing,pp. 335-355, 2006..

[8] Daoud Khadidja, "Propriétés électroniques et élastiques des semi conducteurs anorganiques ", thèse doctorat , université Ferhat Abbas–Setif , 15/03/2012.

[9] S.M. Blinder and J.E. House," Mathematical Physics in Theoretical Chemistry" , Developments in Physical & Theoretical Chemistry, 2019,page7.

[10] W. Pauli, "The Connection Between Spin and Statistics ", American Physical Society,Phys. Rev. 58, 719,1940.

[11] Abdelkarim Soumia, "Etude théorique des réactions de cycloaddition des cétène, thiocétène et sélénocétène avec la formaldimine" , mémoire master, Université d'Oran ,02 / 12 /2009.

[12] Douar Oum el kheir," Etude théorique du pyranne et ses dérivés 2,4-pentadiénals :stabilité et structure moléculaire.", mémoire master, UNIVERSITÉ Dr MOULAY TAHAR – SAÏDA -, 02/07/2017.

[13] Hamada Assia," Etude des propriétés structurales, électroniques et magnétiques du composé binaire CsN", mémoire master, Univesite « Dr. Tahar Moulay » de Saida, 12/06/2019.

[14] N.Troullier and J.L. Martins, "Efficient pseudopotentials for plane-wave calculations", Phys. Rev B 43 (1991) 8861.

[15] L. H. Thomas, "The calculation of atomic fields",Proc. Cambridge Philos, Soc. 23, pp. 542-548,1927.

[16] E. Fermi, Z. "Eine statistische Methode zur Bestimmung einiger Eigenschaften des Atoms und ihre Anwendung auf die Theorie des periodischen Systems der Elemente",Phys. 48,pp73, 1928.

[17] W. Kohn et L. J. Sham, "Self-Consistent Equations Including Exchange and Correlation Effects", Phys. Rev. 140.A1133,1965.

[18] Bedjaoui Abdelhak," Contribution à l'étude des propriétés structurales, élastiques et électroniques des composés AlX (X=N, P et As) " , mémoire magister, Université Ferhat Abbas–Setif ,2011.

[19] P. Hohenberg, W. Kohn, "Inhomogeneous Electron Gas ",Phys. Rev. 136, B864,1964.

[20] W. Kohn, L. Sham, Phys, "Self-Consistent Equations Including Exchange and Correlation Effects", Rev. 140, A1133, 1965.

[21] S. B. Louie, S. Froyen, and M.L. Cohen, Phys. Rev. B 26 (1982) 1738," Nonlinear ionic pseudopotentials in spin-density-functional calculations", Phys. Rev. B 26 (1982),1738.

[22] Merzougui Aicha , "Etude préliminaire de stabilité de défauts ponctuels dans la surface de silicium", mémoire master, Université Mohamed Boudiaf - M'sila, 09 /06/2016.

[23] David S.SHOLL, Janice A.stecked," Density Functional Theory"published by john wiley and sons ,inc, hoboken new jersey ,canada,2009.

[24] Benyettou Samia,"Calcul de premier principe de quelques propriétés physiquesde quelques alliages semi-conducteurs", thèse doctorat, Université Mohamed Khider de Biskra, 04/12/2016.

[25] A. Zaoui and F. Elhadj Hassan, J. Phys, Condens-Matter. 18 (2006) 3647.

[26] P. Giannozzi, S. de Gironcoli, P. Pavone and S. Baroni," Ab initio calculation of phonon dispersions in semiconductors",Phys. Rev. B 43,p7231, 1991.

[27] X. Gonze, First-principles responses of solids to atomic displacements and homogeneous electric fields: Implementation of a conjugate-gradient algorithm, Phys. Rev. B 55,p 10337, 1997.

[28] Souadkia Mourad,"Etude des propriétés vibrationnelles des composés SiGe, SiSn et GeSn ", Mémoire de master, Université de Guelma , 2008.

[29] S.-H. Wei, H. Krakauer, M. Weinert," Linearized augmented-plane-wave calculation of the electronic structure and total energy of tungsten ",Phys. Rev. B 32,p7792, 1985.

[30] V.G. Tyuterev, Nathalie Vast," Murnaghan's equation of state for the electronic ground state energy ", Computational Materials Science 38 (2006) 350–353 .

[31] P. Giannozzi,et al," Quantum Espresso : a modular and open-source software project for quantum simulations of materials", Journal of Physics :Condensed Matter, 21 (2009) 395502 (19pp).

[32] J. M. Soler, E. Artacho, J. D. Gale, et al, "The SIESTA method for ab initio order-N materials simulation", Phys.: Cond. Mat., 14(11) :2745–2779 ,2002.

Chapter III:

Results and discussions.

I. Introduction:

In this chapter, we will present the main part of our modeling and simulation results using the ab-initio method, we made a structural study of aluminum and copper oxide, then built the $AlCu_2O$ model. by changing each time the number of layers and the direction of Al, and calculate the interaction energy between them and then an electronic structure study by mean of the DOS and PDOS curves of the deposited aluminum on the copper oxide.

II. Structural Properties:

II.1. Optimization of calculation parameters:

Before we start the DFT based calculations, it is common to start by optimizing some quantities used by the code and which differ from material to another. In most cases two quantities have to be optimized:

II.1.1.The points-K number of the Brillouin zone:

The number of k points in the first Brillouin zone has a great influence of the time and the precision of the computations. It is used to divide this region in the reciprocal space and calculate different physical quantities by the DFT. We calculated the total energy by changing the number of this points by giving three individual values in the axes (Kx Ky Kz) in the program Quantum Espresso, for the Al and Cu_2O.

- **For Al:**

We vary the values of points- k number, started from the value ((Kx Ky Kz)=(1 1 1) to the value (Kx Ky Kz) =(25 25 25) in the input file, and we draw the curve which represents the total energy as function of the number of points-K as it is indicated by figure:

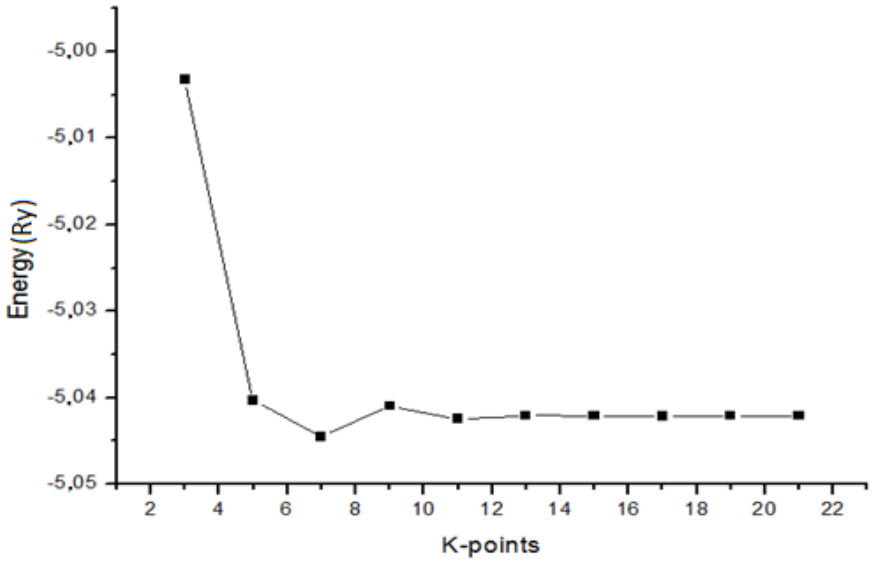

Fig III.1: The total energy of Al mesh as a function of the number of points K.

We notice in the figure III.1 significant fluctuations of the total energy for small values of the number of points-k, and a convergence starting from a value of K=(12 12 12) where the energy undergoes small variations. The value K=(15 15 15) will be used in all following structural calculations that will be studied, because the curve is converged starting from this value corresponding to the minimum energy value.

❖ For Cu_2O:

We changed the number of points-k starting from the value (3 3 3) to the value (27 27 27) in the file input, and extracted the results and put them on the next curve.

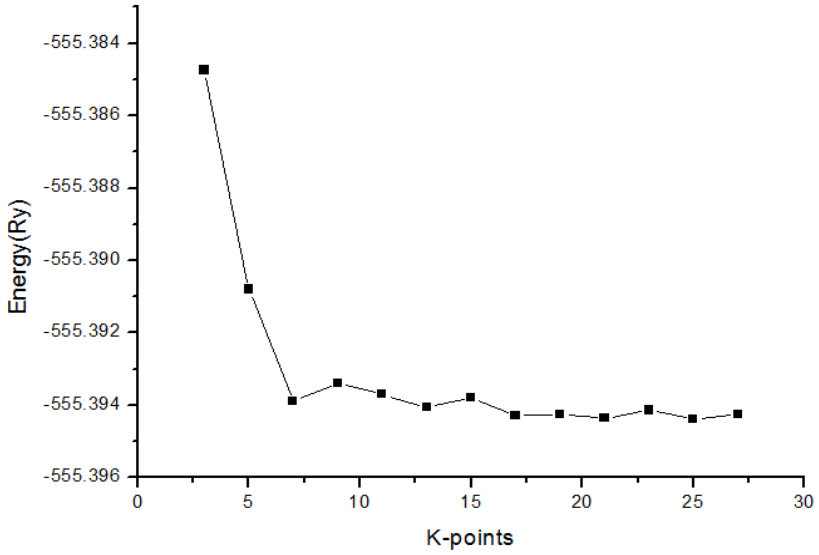

Fig III.2: The total energy of Cu_2O as a function of the number of points K.

The curve (figure III.2) represents the total energy of Cu2O as function of the number of points-K.

Where we notice a decrease in the interval [4-10], and small fluctuation in the energy values after the value 10 for the number of points-K. We choose the value (Kx Ky Kz) = (25 25 25) as the working value.

II.1.2. $E_{cut\text{-}off}$ Energy:

The cutting energy determines the basis the plane waves, and also controls the accuracy and calculation time, it is associated with the kinetic energy of the electrons in the material. To optimize this parameter we have to change the values of $E_{cut\text{-}off}$ in the input file and for each value we calculate the total energy and we plot the variation curve of the total energy as a function of the cut-off energy for the Al and Cu_2O.

❖ **For Al:**

We changed the energy $E_{cut\text{-}off}$ values, from the value of 11 Ry to the last value of 50 Ry. We recorded the results in the following curve:

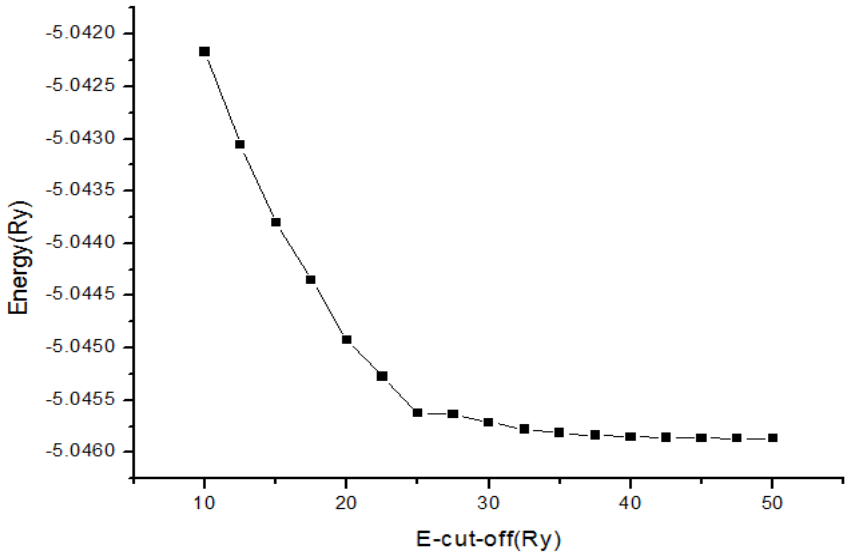

Fig III.3: The total energy of Al mesh as a function of $E_{cut\text{-}off}$.

We did notice in figure III.3, that the total energy converges from the value 25 Ry of $E_{cut\text{-}off}$. We take $E_{cut\text{-}off}$ =32 Ry. This value is used in all calculations of the studied structures.

❖ **For Cu_2O:**

We changed the energy $E_{cut\text{-}off}$ values from the value of 7.5 Ry to the last value of 40 Ry. We recorded the results in the following curve:

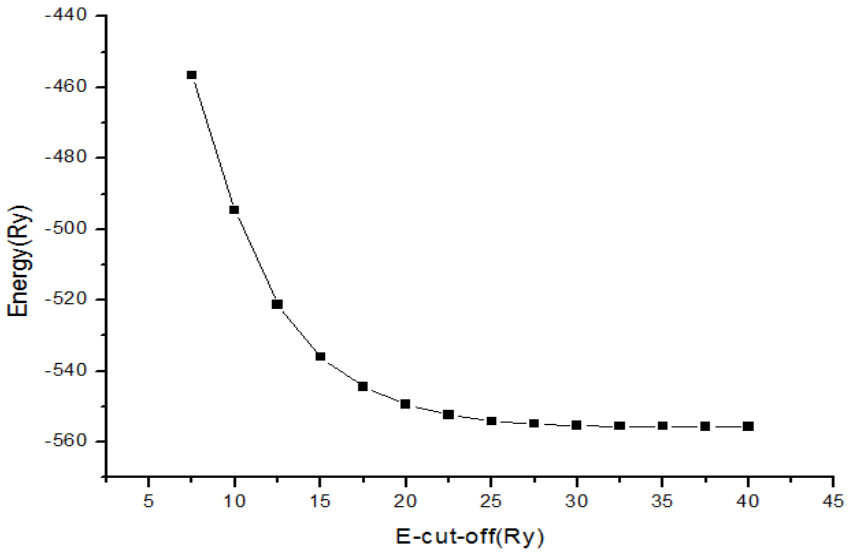

Fig III.4: The total Energy of Cu_2O as a function of energy $E_{cut\text{-}off}$.

The curve (figure III.4) shows that the values of the total energy of Cu_2O is decrease in the interval [10-30] and constant after the value 30. This means that the value $E_{cut\text{-}off}$=30 Ry, corresponding to the lowest value of the total energy of Cu_2O is suitable for the future calculations.

II.1.3.The lattice parameter :

Fixing the value of the $E_{cut\text{-}off}$ energy and the number of points-k, is not sufficient to give the smallest value for the total energy, and on this basis the value of the lattice parameter for Al and Cu_2O must be optimized by changing the cell parameter and calculating the total energy:

➢ **For Al:**

We recorded the results of calculation and placed them in the following curve:

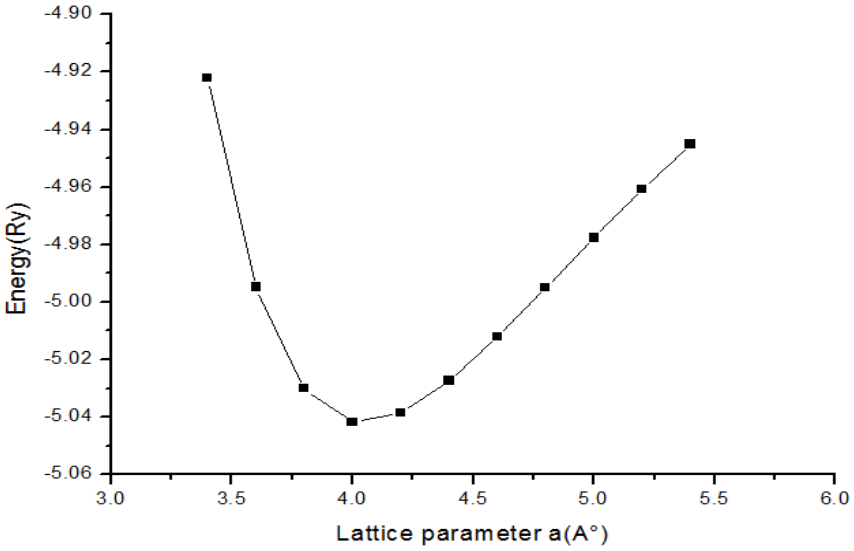

Fig III.5: The total Energy of Al as a function of the lattice parameter a_{Al}.

The curve (figure III.5) represents the total energy values of Al unit cell as function of the lattice parameter a. We take the value $a_{Al} = 4.01A°$, as a reference value at which the system reaches its lowest energy, which agreement of experimental and theoretical values [1, 2].

❖ **For Cu_2O:**

We recorded the results and placed them in the following curve:

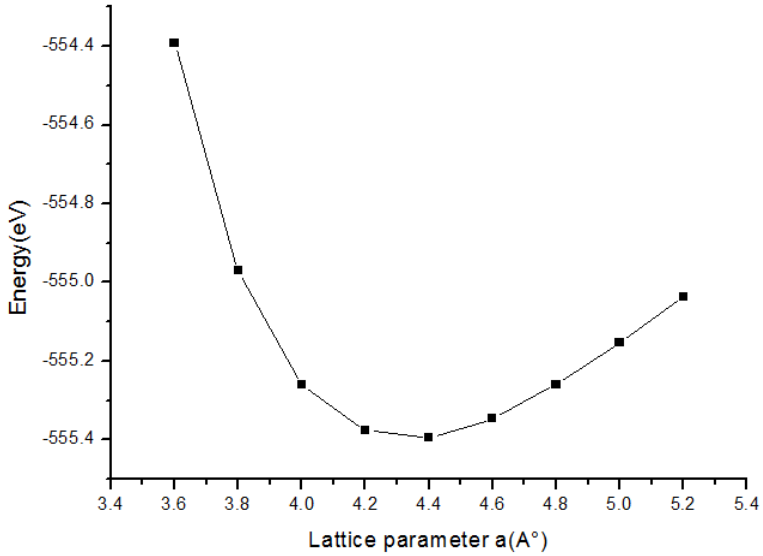

Fig III.6: The total Energy of Cu_2O as a function of the lattice parameter a_{Cu2O}.

The curve (figure III.6) represents the total energy of Cu_2O unit cell as function of the lattice parameter, where we note that the value of the lattice parameter a corresponding to the

lowest total energy is $a_{Cu_2O} = 4.363\,A°$, for accuracy this value is used in all calculations, which agreement of experimental and theoretical values [3,4].

II.1.4. Fitting to Murnaghan equation of state:

The total energy of our material Cu_2O and Al, is calculated as a function of volume. A fit of these results according to the Murnaghan equation [5] was performed. From this fit, we were able to determine the equilibrium lattice parameter a_0, and the compression modulus B_0 at zero pressure. Our calculated values of these parameters are shown in the following curve for aluminum and copper oxide:

- **For Al:**

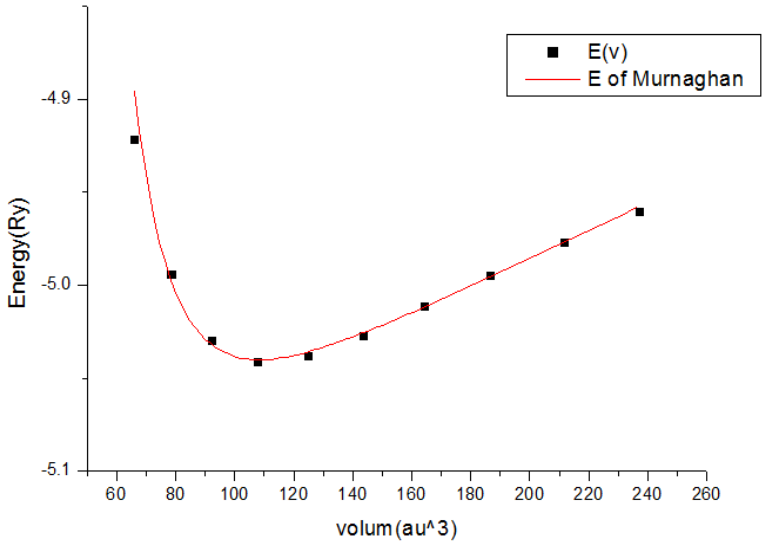

Fig III.7: Total energy as a function of volume for Al.

In figure III.7, we have plotted the total energy of the system as a function of the volume of the cell.

The lowest energy state corresponds to the equilibrium state at V_0=433.324 au^3. and The minimum of the curve corresponds to the lattice parameter of the material at a_0 = 4.003 A° (which is very close to that taken from the minimum of total energy vs lattice parameter), and it is close to the experimental value (4.05 A°), and calculated in other theoretical works (4.05 A°) [6]. The value of the bulk modulus (which expresses the compressibility factor of the

material) β=55.6 GPa , it is close to the experimental value (81.13 GPa), and calculated in other theoretical works (80.2 GPa) [6].

Note:

The PW code uses fcc symetry, so the unit cell volume is ¼ of a^3.

❖ **For Cu_2O:**

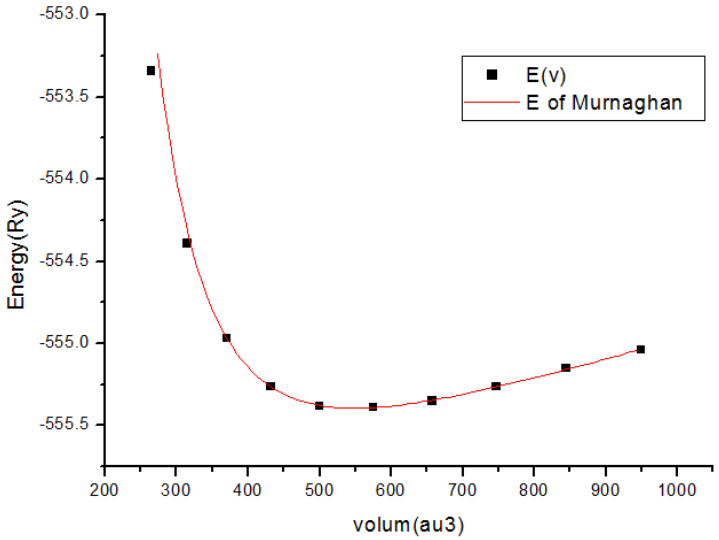

Fig III.8: Total energy as a function of volume for Cu_2O.

In Fig III.8, we have plotted the total energy of the system as a function of the volume of the cell. The lowest energy state corresponds to the equilibrium state at V_0=81.2668 A°^{3}. The minimum of the curve corresponds to the lattice parameter of the material at a_0=4.332 A°(which is very close to that taken from the minimum of total energy vs lattice parameter), and it is close to the experimental value (4.27 A°) and calculated in other theoretical works (4.312 A°) [7].
The value of the bulk modulus β=90.815 GPa, it is close to the experimental value (112 GPa) and calculated in other theoretical works (118 GPa) [8,9].

III.Modeling Al(001)/Cu_2O(001) interface:

A model for this interface to be used as a unit cell has been created by DFT code. This unit cell should contain the two substances that we intend to search for interaction energy between them. The model is constructed as follows: a number of unit cells of aluminum are placed over another number of unit cells of copper oxide so that the unit cell matches the first and last atoms of both materials, to achieve this matching, a certain number of layers must be found for the copper oxide material, which

must correspond to a certain number of layers of aluminum material, the presence of a large number of layers increases the calculation time, in this case we resort to another method represented by a small dilatation or reducing in the surface lattice parameter for the material that has a less compressibility (the dilatation must be less than 10%), in order to be equal to the other lattice parameter to reach the desired matching. As a result of this dilatation, the atoms of the material are not in equilibrium state, a situation that must be corrected by finding the c parameter by searching the lowest energy of a dilated cubic fcc unit cell along and b directions.

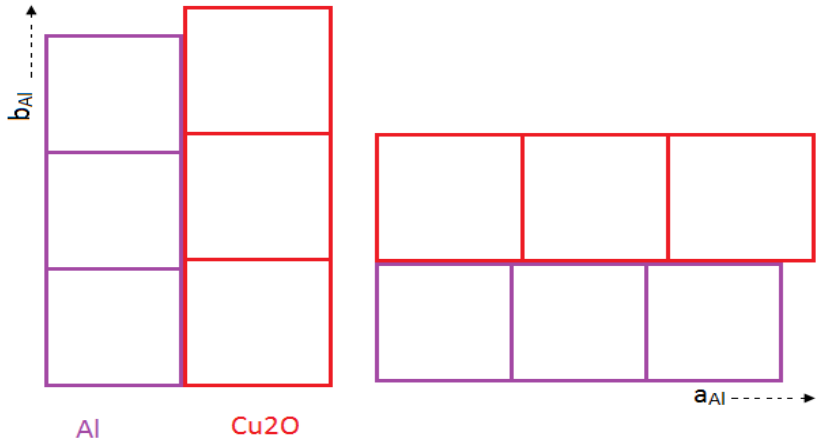

Fig III.9: An illustration of the expansion in the studied material.

III.1. The mismatch:

We calculate the mismatch between the surface atoms of aluminum Al and copper oxide Cu_2O in the direction <001>. And this is by applying the following relation:

$$|a_{Al}M - a_{Cu2o}N| \leq 0.1\ A° \qquad (1)$$

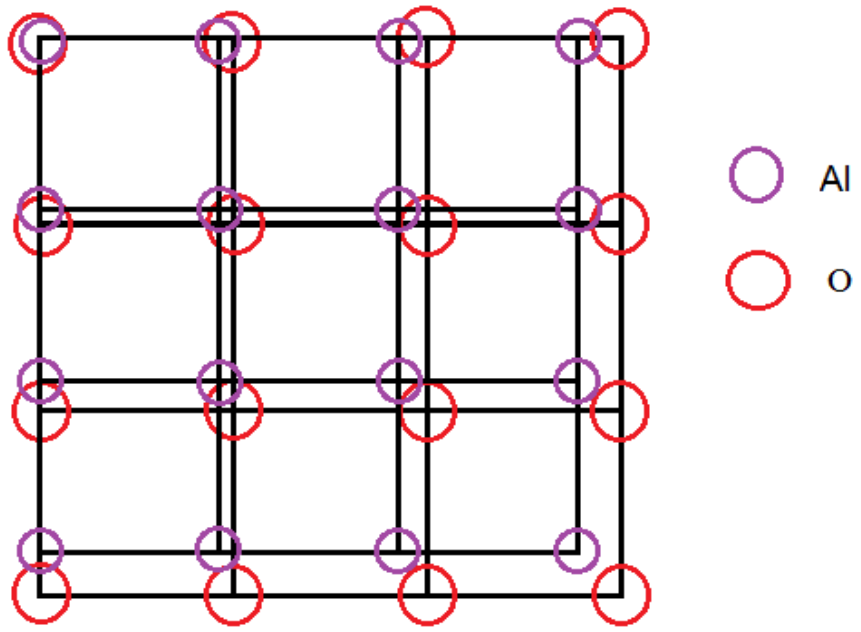

Fig III.10: Mismatch of $AlCu_2O$ in direction <001>.

M and N represents the number of unit cells of aluminum and copper oxide. Respectively, this must correspond to a given number to achieve the congruency (matching) relation.

In this case, we found that the previous relation (1) is achieved at M =12 and N =11 (large number of unit cells), since the value of the aluminum lattice parameter a_{Al} is not far from close to the value of the copper oxide lattice parameter a_{Cu_2O}, we did a small dilatation in the lattice parameter of the aluminum surface a_{Al} and b_{Al} so that they are to equal a_{Cu_2O} (we chose aluminum because it is easy to dilate since $\beta_{Al} < \beta_{Cu_2O}$). Dilating the aluminum must be corrected by finding the c parameter by searching the lowest energy of a dilated cubic fcc unit cell along and b directions.

III.2.Lattice parameter c_{Al} :

We find c_{Al} by changing its values, and calculating the energy at each value. We put the results in the following curve:

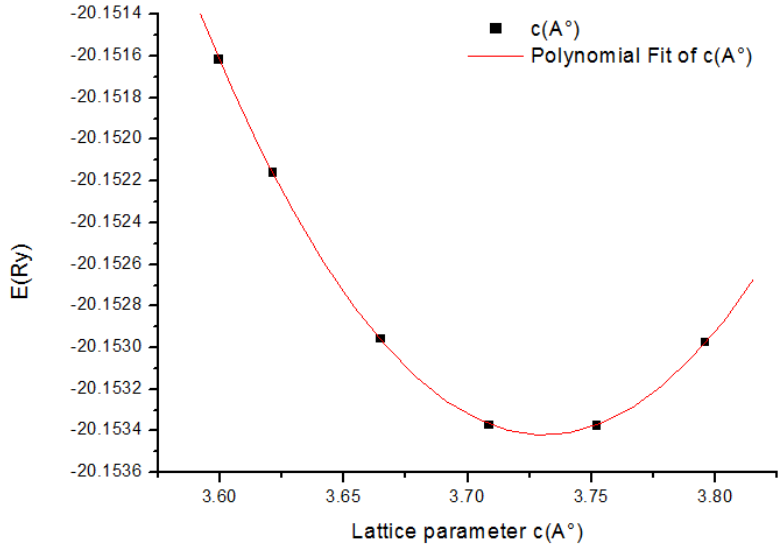

Fig III.11: The total energy values of the system as a function of lattice parameter c($A°$) for the model Al(001)Cu_2O.

We note from the curve (figure III.11) :

Decreases in the interval [3.60-3.73] and increases in the interval [3.73-3.80].

From the fit (the curve red), we extracted the equation of a second-degree polynomial, then we derive it and found the value of c:

$$E = 1.72233c^2 - 2.9433c - 18.8957$$

$$c_0 = 3.7306\ A°$$

This value corresponds to the smallest total energy of the system at which it reaches stability. It is used for the rest of the following calculations.

III.3. The model Al(001)Cu_2O (1 layer of Aluminum and 1 layer of Copper Oxide):

II.3.1.Interaction of system Al(001)Cu_2O:

The next figure represents the model $AlCu_2O$ in the direction <001> (1 layer of aluminum and 1 layer of copper oxide).

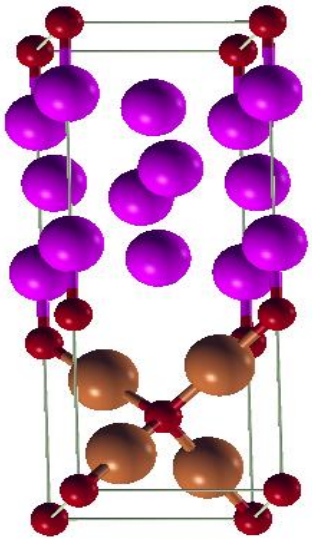

Fig III.12: The model of Al(001)Cu_2O (1 layer of Al and 1 layer of Cu_2O).

II.3.2.The distance between of layers d:

We change the values of d (the distance between layers of Al and Cu2O) to find a value for the smallest total energy.

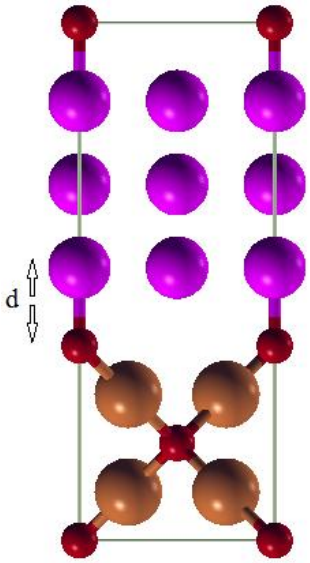

Fig III.13: The distance between the Al and Cu_2O layers.

Where we calculate starting from the value d =1.65 to the value d =1.85 in a file input, then extract the results from File output and put it in the following curve:

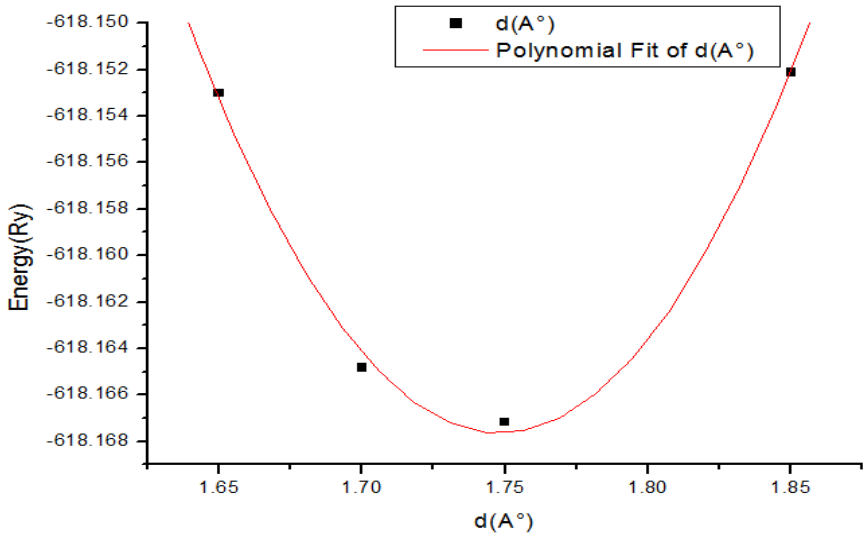

Fig III.14: The total energy values of the system Al (001)Cu_2O (1 layer of Al and 1 layer of Cu2O) as a function of the distance between layers Al and Cu_2O.

The curve (figure III.14) represents the total energy values of the system AlCu2O as a function of the distance d, we notice that the total energy decreases in the interval [1.655-1.75] and increases in the interval [1.75-1.85].

From the fit (the curve red), we extracted the equation of a second-degree polynomial, and then we derive it and found the value of d_0:

$$E = 1.49991d^2 - 5.24356d - 613.585$$

We find d_0=1.748$A°$ is the smallest possible for the total energy and the system is stable.

III.3.3.Adhesion energy E_{ad} of the model $AlCu_2O$:

The energy of adhesion E_{ad} is defined as the energy needed to separate the surfaces that conform the interface in terms of surface area [10].

The energy of adhesion is expressed by the following law:

$$E_{ad} = \frac{(E_{AlCu_2O} - E_{Cu_2O} - E_{Al})}{2A}$$

E_{ad}: Adhesion energy

E_{AlCu2O}: Energy total of system ($AlCu_2O$).

A: the surface contact area.

E_{Cu2O}:Energy of system (Cu_2O+ vacuum).

E_{Al}: Energy of system (Al+ vacuum).

After finding the value of d. We prove it and then build the model at this value, then calculate the total energy of the system $AlCu_2O$ where we find its value $E_{AlCu_2O} = -8410.574810116ev$.

II.3.3.1.Interaction of system Al with vacuum:

Fig III.15: Model (Al+vacuum) in direction <001>.

We calculate the total energy of the aluminum system with the vacuum (we canceling the copper and oxygen atoms).we finds the energy value there $E_{Al} = -408.919085437ev$.

III.3.3.2.Interaction of system Cu_2O with vacuum:

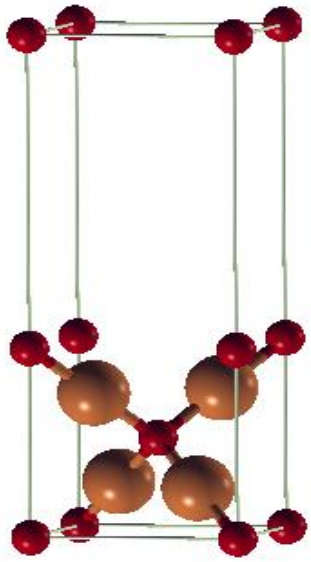

Fig III.16: The model (Cu_2O+vacuum) in direction <001>.

We calculate the total energy of the system copper oxide with vacuum (we canceling the aluminum atoms). Where we find the energy in it $E_{Cu_2O} = -7996.017882043ev$.

III.3.3.3.Calculate the energy of adhesion:

We substitute the previous values in the law. We find the energy of adhesion:

$$E_{ad} = \frac{(-8410.574810116+7996.017882043+408.919085437)}{2*19.0358} \quad \Longrightarrow \quad E_{ad1} = -0.148085\ eV/\text{A}^{\circ 2}$$

We Note that $E_{ad1} < 0$. This indicates the presence of adhesion between the aluminum and copper oxide layers.

III.4 .The model Al(001)Cu_2O (2 layers of Al with 2 layers of Cu_2O):

III.4.1. Interaction of system Al(001)Cu_2O:

The next figure represents the model AlCu_2O in the direction <001> (2 layers of aluminum and 2 layers of copper oxide).

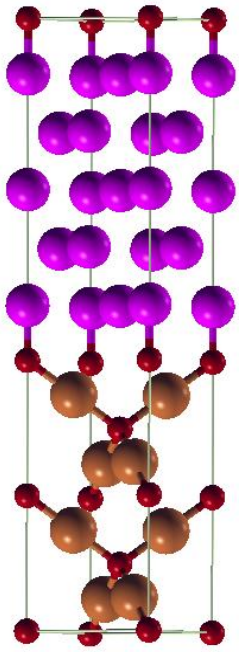

Fig III.17: The model of Al(001)Cu_2O (2 layers of Al and 2 layers of Cu_2O).

III.4.2. The distance between of layers d:

The next curve represents the total energy values of the system $AlCu_2O$ as a function of the distance between layers Al and Cu_2O.

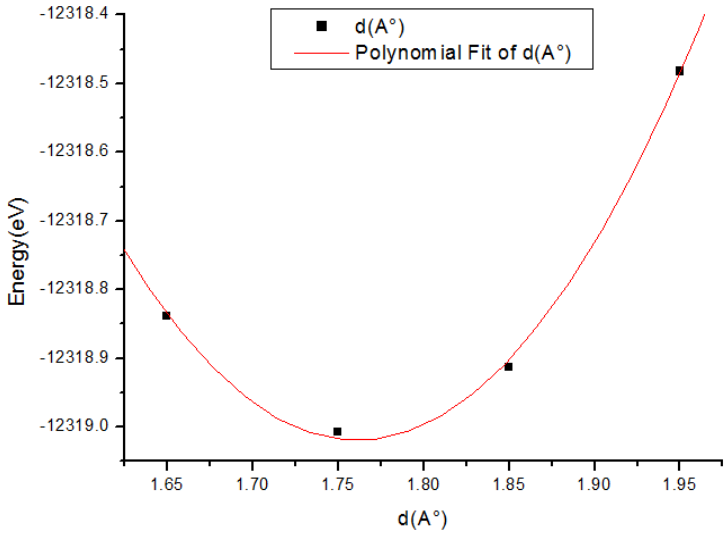

Fig III.18: The total energy values of the system Al(001)Cu_2O (2 layers of Al and 2 layers of Cu_2O) as a function of the distance between layers Al and Cu_2O.

We notice in figure III.18 that the total energy decreases in the interval [1.65-1.75] and increases in the interval [1.75-1.95].

From the fit (the red curve), we extracted the equation of a second-degree polynomial, then we derive it and found the value of d:

$$E = 14.9725d^2 - 52.7363d - 12272.58299$$

We find d_0=1.7611$A°$ is the smallest possible for the total energy and the system is stable**.**

III.4.3.Adhesion energy E_{ad} of the model $AlCu_2O$:

The energy of adhesion is expressed by the following law:

$$E_{ad} = \frac{(E_{AlCu_2O} - E_{Cu_2O} - E_{Al})}{2A}$$

After finding the value of d_0. We prove it and then build the model at this value, then calculate the total energy of the system $AlCu_2O$ where we find its value $E_{AlCu_2O} = -12319.0702eV$, then we calculate the energy of the system copper oxide with vacuum (we canceling the aluminum atoms) where we find the energy in it $E_{Cu_2O} = -11750.2706eV$, and we calculate the energy of the aluminum system with the vacuum (we canceling the copper and oxygen atoms), we find the energy value there $E_{Al} = -560.8038eV$.

We substitute the previous values in the law. We find the energy of adhesion:

$$E_{ad2} - 0.10496 \ eV/A^{\circ 2}$$

We note that $E_{ad2} < 0$. This indicates the presence of adhesion between the aluminum and copper oxide layers.

We concluded that the adhesion is good in the model with two layers of aluminum and two layers of copper oxide because $E_{ad2} < E_{ad1}$.

III .5.The nearest neighbor to the Aluminum atom:

After constructing the model $AlCu_2O$ each aluminum atom is characterized by a the nearest neighbors to it from the surface that expresses the extent of adhesion with copper oxide, as this is determined based on the crystalline distance between the two aluminum and oxygen atoms by estimating the smallest distance between them. The smaller the distance and greater the number of nearest neighbors, the better the bond between the atoms and the better the adhesion in the more layered model.

We calculated the distance of the nearest neighbors and the number of nearest neighbors for the two models with regarding to the oxygen atoms with the surface aluminum atoms.

- **For the model Al/Cu_2O {2 layers of Al and 2 layers of Cu_2O} in the <001> direction:**

We found that the closest distance is the value $d_{(Al\_O)}$ = 1.7611A° and that the number of nearest neighbors is 1.

- **For the model Al /Cu_2O {1 layer of Al and 1 layer of Cu_2O} in the <001> direction:**

We found that the closest distance is the value $d_{(Al\_O)}$ = 1.748A° and that the number of nearest neighbors is 1.

We observed a convergence in the values of the nearest neighbors between the two models, while the nearest neighbors of the two-layer model must be less than the one-layer models. However, we see that this difference is estimated to be 0.01A°, i.e. negligible in atomic dimensions. This may be due to a error of calculations, or interpolation in the system, or due to approximations used in the input file.

IV. Modeling Al (111)/Cu_2O(001) interface:

To create this model, we follow the same steps aforementioned, starting with:

IV.1. The mismatch:

Since the aluminum parameter is not cubed (a ≠b), the relation 1 will be calculated in both directions:

- **Direction x:**

We found that:

N=13 and M=20 (large numbers). So we matched 3 layers of Aluminum and 2 layers of Cu_2O with a small dilatation of aluminum lattice parameter a_{Al}, so that a_{Al}=2.91 A° .

- **Direction y:**

We found :

N=9 and M=8 (large numbers).

We matched one layers of Aluminum and one layers of Cu_2O with a curtailment in the aluminum lattice parameter b_{Al} so that they are to equal a_{Cu_2O} :

$$b_{Al} = a_{Cu_2O} = 4.363 \text{ A°}.$$

Thus, we achieved matching the interface of the model Al(111)Cu_2O(001).

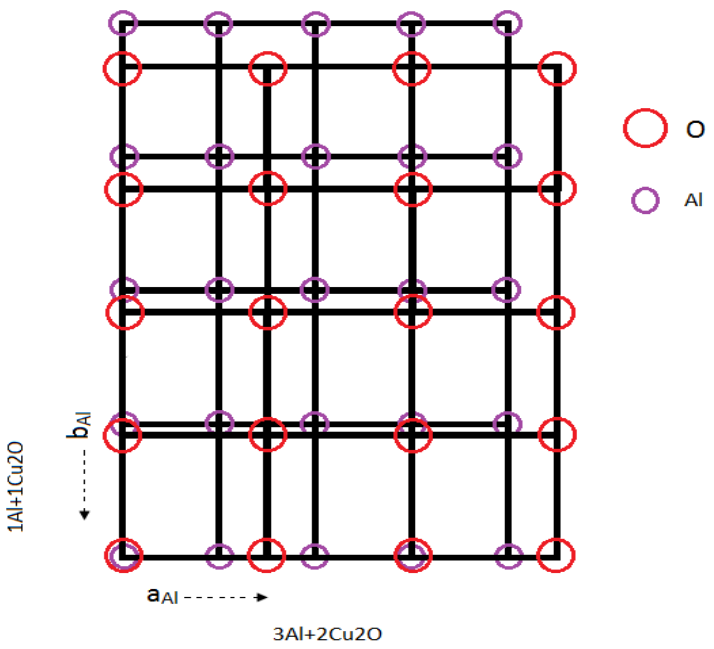

Fig III.19: Mismatch of Al(111)Cu_2O.

IV.2.Lattice parameter c:

In order to find the mesh parameters c of our structure in a numerical way we start by varying the parameter c from 7.3 A° to 7.7A°.

The parameter c of the calculated network c are represented in Fig III.20.

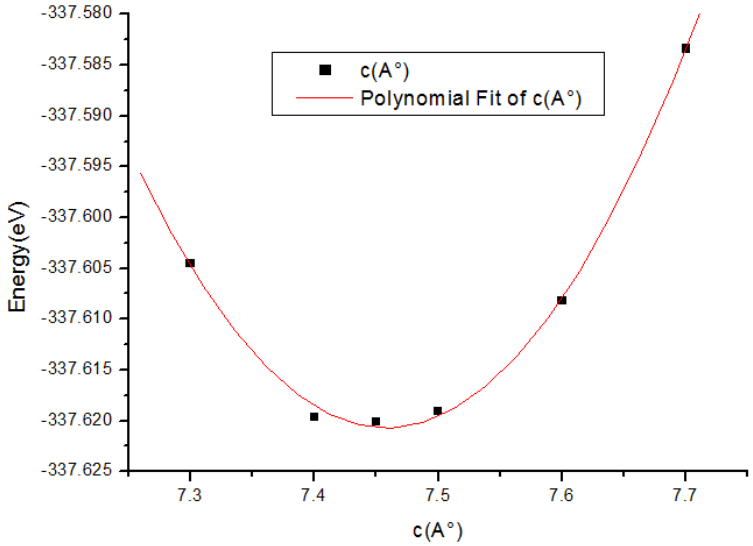

Fig III.20: Variation of the total energy as a function of c(A°) for the distorted aluminum.

from the curve:

We note decreases in the interval [7.3-7.467] and increases in the interval [7.467-7.7].

From the fit (the curve red), we extracted the equation of a second-degree polynomial, then we derive it and found the value of c:

$$E = 0.75109c^2 - 11.3175c - 295.73904$$

$$c_0 = 7.467\ A°$$

This value corresponds to the smallest total energy of the system at which it reaches stability. It is used for the rest of the following calculations.

IV.3.The model Al(111)Cu_2O (1 layer of Al and 2 layers of Cu_2O):

IV.3.1.Interaction of system AlCu_2O:

The next figure represents the model Al(111)Cu_2O (1 layer of Al and 2 layers of Cu_2O).

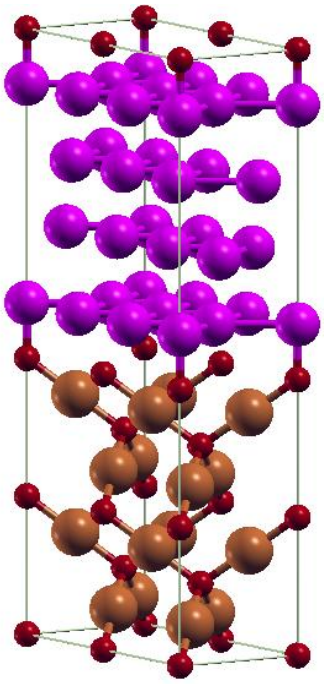

Fig III.21: The model of Al(111)Cu_2O (1 layer of Al and 2 layers of Cu_2O).

IV.3.2. The distance between of layers d:

As we did in the previous models, we research for d the distance between the layers of Al and Cu_2O, and then we represent in the curve the total energy of the system Al(111) Cu_2O as a function of the distance d, show in figure III.22.

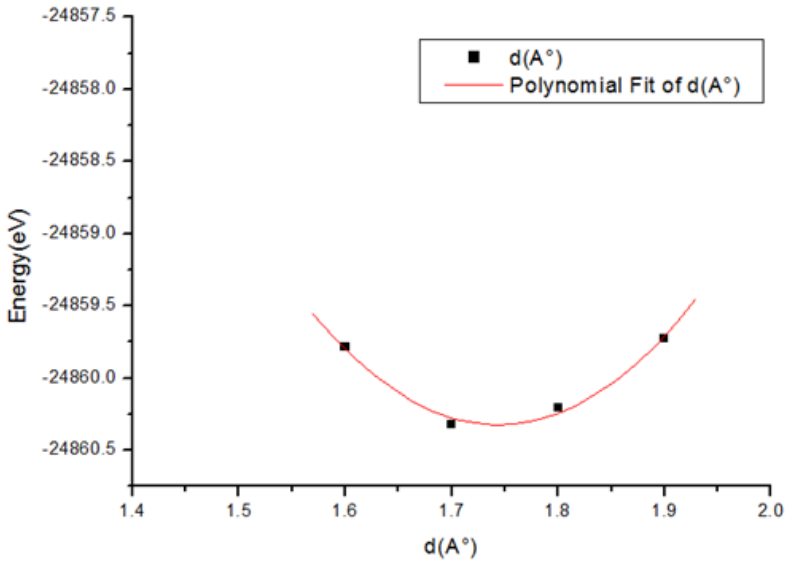

Fig III.22: The total energy values of the system Al(111)Cu_2O as a function of the distance between Al and Cu_2O.

From the fit (the red curve), we extracted the equation of a second-degree polynomial, then we derive it and found the value of d:

$$E(d) = 25.4025d^2 - 88.60925d - 24783.05477$$

We find d_0=1.744 $A°$ is the smallest possible for the total energy and the system is stable.

IV.3.3.Adhesion energy E_{ad} of the model $AlCu_2O$:

After finding the value of d_0. We prove it and then build the model at this value, then calculate the total energy of the system $AlCu_2O$ where we find its value $E_{AlCu_2O} = -24860.3822eV$. Then we calculate the energy of the system copper oxide with vacuum (we canceling the aluminum atoms) where we find the energy in it $E_{Cu_2O} = -23500.5334eV$. And we calculate the energy of the aluminum system with the vacuum (we canceling the copper and oxygen atoms), we find the energy value there $E_{Al} = -1345.8569eV$. We substitute these values into the following law to find the energy of adhesion:

$$E_{ad} = \frac{(E_{AlCu_2O} - E_{Cu_2O} - E_{Al})}{2A}$$

$$E_{ad3} = -0.18367\ eV/A^{\circ 2}$$

We note that E_{ad3}<0 ,this indicates the presence of adhesion between the aluminum and copper oxide layers.

From the comparison of the two models (Al(111) Cu_2O with Al(001)Cu_2O (2 layers of Al and 2 layers of Cu_2O), we conclude that the adhesion in the Al (111)Cu_2O model is better ($E_{ad3} < E_{ad2}$). The comparison do not include the Al(001)Cu_2O (1 layer of Al and 1 layer of Cu_2O) because it contains less atomic layers for aluminum and copper oxide.

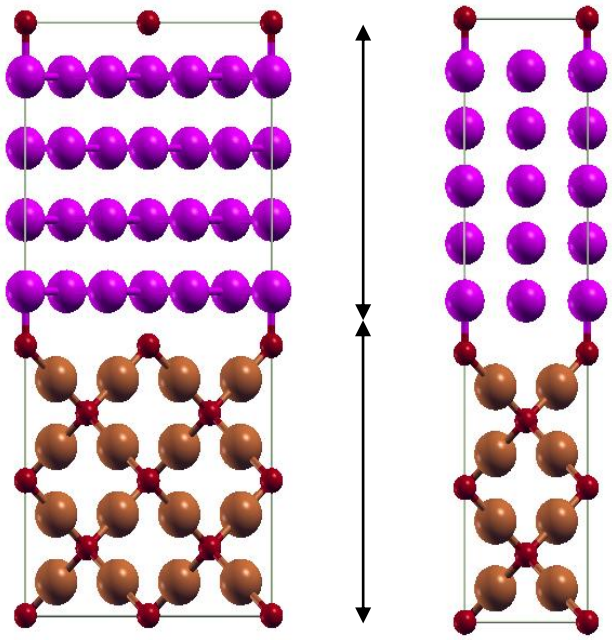

Fig III.23: An illustration showing the atomic layers of aluminum and copper oxide for the two models.

V. The electronic properties:

V.1. Density of states (DOS) and Projected density of states (PDOS):

The density of electronic states is a major factor in condensed matter physics and materials science, and it is one of the most important electronic properties that tell about a systems electronic character. It also allows us to know the nature of the chemical bonds between the atoms of a crystal or a molecule.

In our case, we studied the PDOS qualitatively, by comparing between atoms orbitals and comparing the two models (Al(111)Cu_2O (one layer of Al and two layers of Cu_2O) and Al(001)Cu_2O (two layers of Al and two layers of Cu_2O), so whenever the greater the number of congruent orbital's, adhesion becomes better and the bond between the atoms stronger.

From the curve of projected density of states (PDOS) we can know the Prevailing character of each region as well as the electronic states that contribute to the peaks , as they are deduced from the total density of state (DOS) projected onto the atomic orbits of each compound (s, p, d states).

The 4s and 4p orbitals of the two Cu atoms do not contribute to the interaction between the Al and Cu_2O layer. As a check, PDOS calculations were performed on the 4s and 4p orbits of the Cu atoms, and found that all of these projections were very weak in intensity.

V.1.1. For Al(100)Cu_2O {2 layers of Al and 2 layers of Cu_2O}:

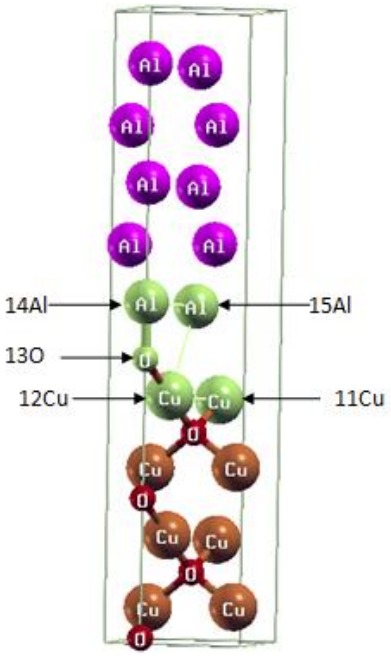

Fig III.24: An illustration showing the interface atoms of the model Al(001)Cu_2O(2 layers of Al and 2 layers of Cu_2O).

We calculated the total and molecular density of the Al(001)Cu_2O states in terms of energy and were recorded in the following curves:

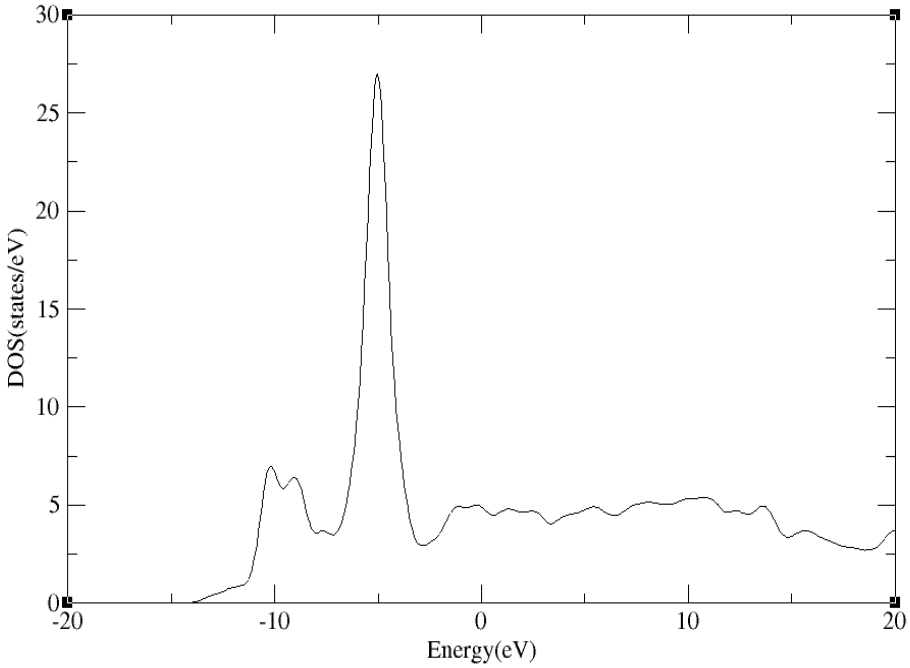

Fig III.25: Density of total states of the model Al(001)Cu_2O(2 layers of Al and 2 layers of Cu_2O).

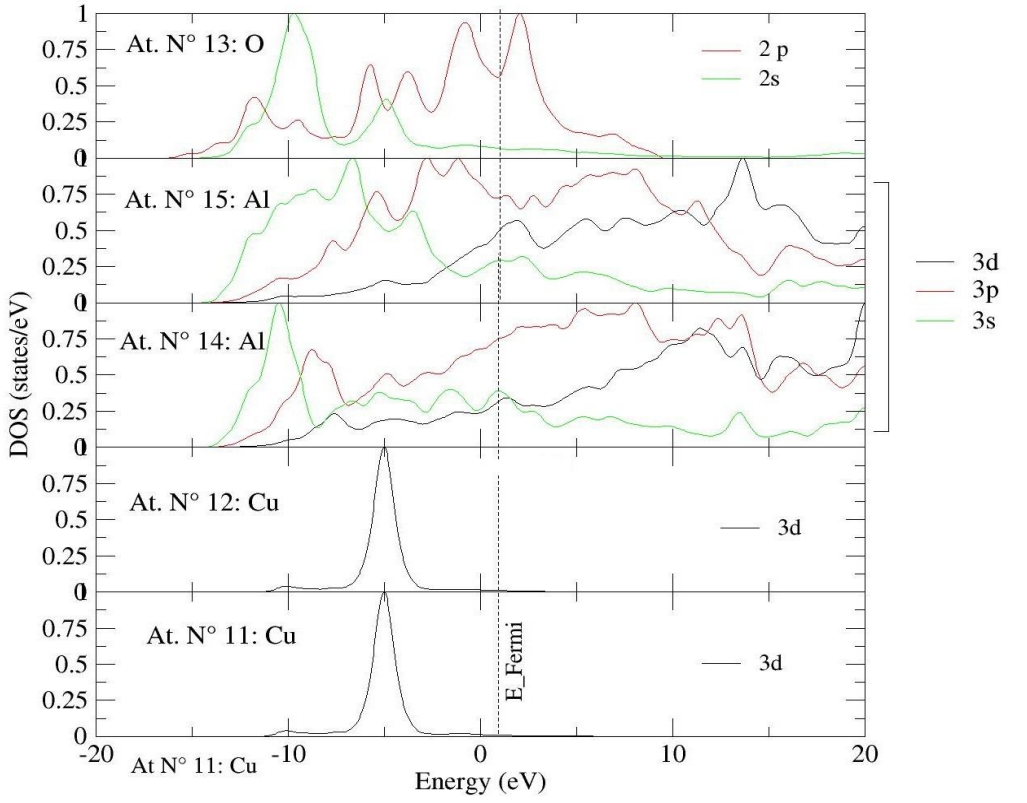

Fig III.26: Projected density of states of the model Al(001)Cu_2O(2 layers of Al and 2 layers of Cu_2O).

Since we have studied the qualitative curves of PDOS, we did resort to dividing the curve of each orbit by its highest peak value in order to minimize the curve. We put Subdivisions values in the following table:

Orbital	**$PDOS_{max}$[states/eV]**
At. N° 13:O 2s	0.01
At. N° 13:O 2p	0.641
At. N° 15:Al 3s	0.095
At. N° 15:Al 3p	0.191
At. N° 15:Al 3d	0.345
At. N° 14:Al 3s	0.112
At. N° 14:Al 3p	0. 175
At. N° 14:Al 3d	0.265
At. N° 12:Cu 3d	3.023
At. N° 11:Cu 3d	3.023

Table III.1: Subdivisions values of orbitals position for the model Al(001)Cu_2O(2 layers of Al and 2 layers of Cu_2O).

$[-3,1]$ There is a match between the oxygen atom 13 for the 2p orbital with an aluminum atom 15 for the 3p orbital and an aluminum atom 14 for the 3s orbital.

$[-3,-5]$There is a match between the oxygen atoms 13 for the 2p orbital with an aluminum atom 15 for the orbital 3s and for the aluminum atom for the 3s orbital.

$[-3.5,-8]$ There is a match between the oxygen atom 13 for the 2s orbital with an aluminum atom 15 for the 3p orbital and in the same atom for the 3d orbital with an aluminum atom 14 for the 3p orbital and for the 3d orbital and for the 3s orbital.

$[-3.5,-8]$ There is a match between the aluminum atom 15 for the 3p orbital with an aluminum atom 14 for the 3p orbital and in the same atom for the 3s orbital and for the 3d orbital with an copper atoms 11 and 12 for the 3d orbital.

$[-5,-7.5]$ There is a match between the oxygen atoms 13 for the 2p orbital with an aluminum atom 15 for the 3p orbital.

$[-7.5, -11.5]$ There is a match between the oxygen atom 13 for the 2s orbital and in the same atom for the 2p orbital, with an aluminum atom 14 for the 3s orbital.

$[-10, -13.5]$ There is a match between the oxygen atom 13 for the 2p orbital with an aluminum atom 15 for the orbital 3s.

We Conclude from our analysis of the PDOS (001) curves that the two interval$[-3.5, -8]$; $[-10, -13.5]$ include the highest and lowest orbitals from the Fermi level. This indicates the existence of a strong atomic bond (the higher and farther the peak is from the Fermi level, the better the bond between the atoms).

V.1.2. For Al(111)Cu_2O (1 layer of Al and 2 layers of Cu_2O):

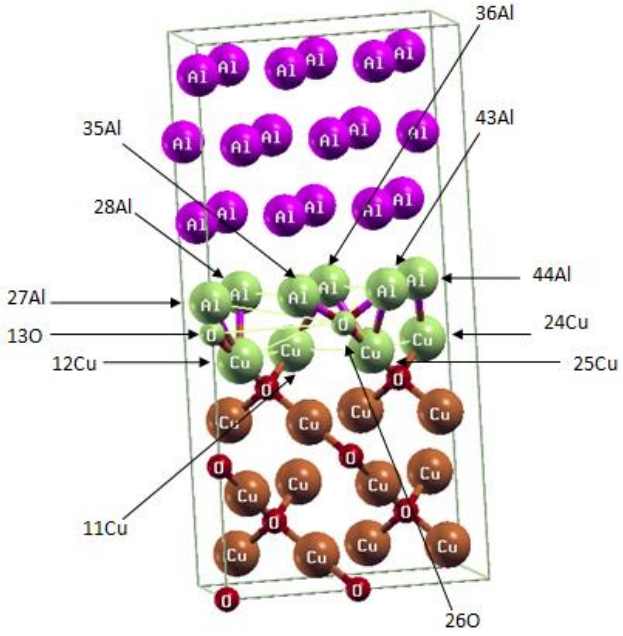

Fig III.27: An illustration showing the interface atoms of the model Al(111)Cu_2O(1 layer of Al and 2 layers of Cu_2O).

We calculated the total and molecular density of the Al(111)Cu_2O states in terms of energy and were recorded in the following curves:

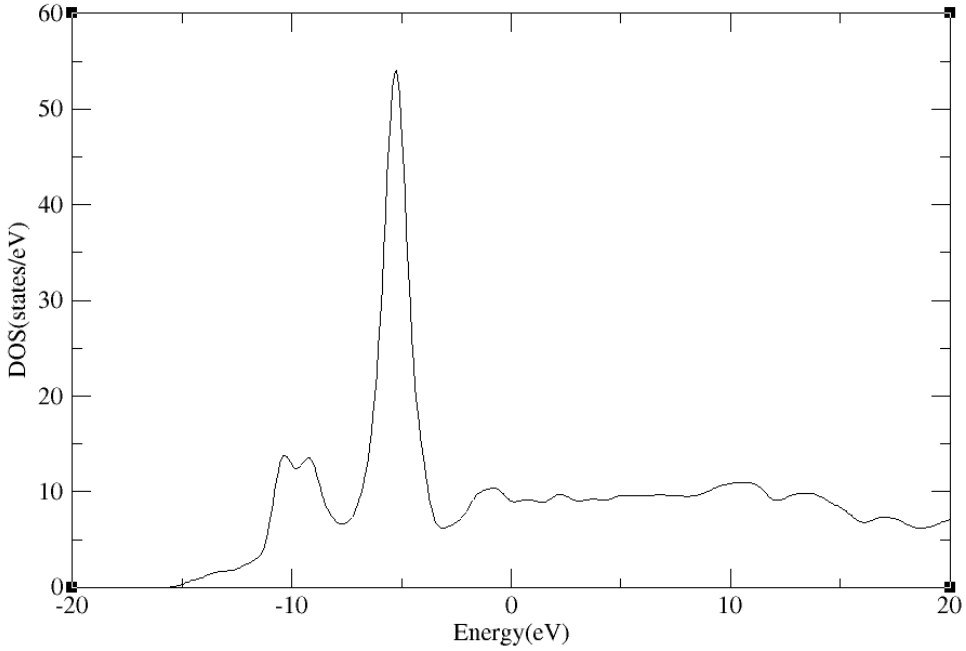

Fig III.28: Density of states of the model Al(111)Cu_2O(1 layers of Al and 2 layers of Cu_2O).

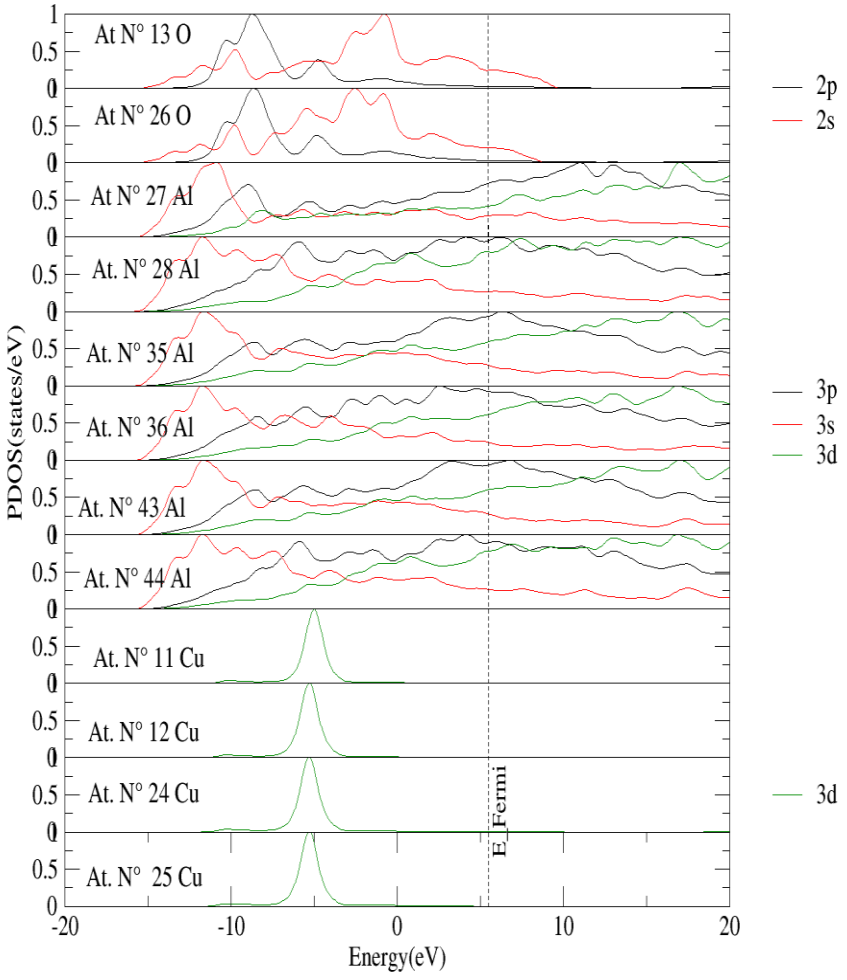

Fig III.29: Projected density of states of the model Al(111)Cu_2O(1 layer of Al and 2 layers of Cu_2O).

Orbital	$PDOS_{max}$[states/eV]
At. N° 13:O 2s	0.009118
At. N° 13:O 2p	0.607856
At. N° 26:O 2s	0.008387
At. N° 26:O 2p	0.632087
At. N° 27:Al 3s	0.074232
At. N° 27:Al 3p	0.159547
At. N° 27:Al 3d	0. 223555
At. N° 28:Al 3s	0.066420
At. N° 28:Al 3p	0.134556
At. N° 28:Al 3d	0.179355
At. N° 35:Al 3s	0.071894
At. N° 35:Al 3p	0.151907
At. N° 35:Al 3d	0.209533
At. N° 36:Al 3s	0.072587
At. N° 36:Al 3p	0.142281
At. N° 36:Al 3d	0.211990
At. N° 43:Al 3s	0.071879
At. N° 43:Al 3p	0.146368
At. N° 43:Al 3d	0.215499
At. N° 44:Al 3s	0.066294
At. N° 44:Al 3p	0.140810
At. N° 44:Al 3d	0.191035
At. N° 11:Cu 3d	2.966010
At. N° 12:Cu 3d	2.941020
At. N° 24:Cu 3d	2.946520
At. N° 25:Cu 3d	0.979400

Table III.2: Subdivisions values of orbital's position for the model Al(111)Cu_2O(1 layer of Al and 2 layers of Cu_2O).

[5.03, −1.32] There is a match at the peaks of the oxygen atom 13 for the 2s orbital with the aluminum atom N° 35 for the 3d orbital and the aluminum atom N° 36 for the 3p orbital and the aluminum atom N° 43 for the 3p orbital.

[2.96, 1.27] There is a match at the peaks of the oxygen atom N° 26 for the 2s orbital with the aluminum atom N° 36 for the 3s orbital and an aluminum atom N° 44 for the 3s.

[0.37, −1.80] There is a match at the peaks of the oxygen atom N°13 for the 2s and oxygen atom 26 for the 2s orbital with the aluminum atom N° 27 for the 3p orbital and the aluminum atom N° 28 for the 3s orbital and the aluminum atom N° 35 for the 3d orbital and the aluminum atom N°36 for the 3p orbital.

[−1.85, −3.60] There is a match at the peaks of the oxygen atom N° 13 for the 2s orbital and the oxygen atom N° 26 for the 2s orbital with the aluminum atom N° 27 for the 3p orbital and the aluminum atom N° 27 for the 3s orbital and the aluminum atom N° 28 for the 3p orbital and the aluminum atom N° 35 for the 3d orbital and the aluminum atom N° 36 for the 3p orbital and the aluminum atom N° 43 for the 3p orbital and the aluminum atom N° 44 for the 3p orbital.

[−3.39, −6.26] There is a match at the peaks of the oxygen atom N° 13 for the 2p and oxygen atom N° 26 for the 2p orbital with the aluminum atom N° 28 for the 3s orbital and the aluminum atom N° 35 for the 3d orbital and the aluminum atom N° 36 for the 3s orbital and the aluminum atom N° 44 for the 3s orbital.

[−4.55, −6.14] There is a match at the peaks of the oxygen atom N° 26 for the 2s with the aluminum atom N° 27 for the 3s orbital and the aluminum atom N° 28 for the 3p orbital and the aluminum atom N° 35 for the 3d orbital and the aluminum atom N° 36 for the 3p orbital and the aluminum atom N° 43 for the 3p orbital and the aluminum atom N° 44 for the 3p orbital.

[−6.25, −9.75] There is a match at the peaks of the O atom N° 13 for the 2p and the O atom N° 26 for the 2p with the Al atom N° 27 for the 3p orbital and the Al atom N° 35 for the 3d orbital and the Al atom N° 36 for the 3p orbital.

[−8.53, −10.75] There is a match at the peaks of the O atom N° 13 for the 2s and the O atom N° 26 for the 2s with the Al atom N° 28 for the 3s orbital and the Al atom N° 36 for the 3s orbital and the Al atom N° 44 for the 3s orbital.

[−10.75, −12.77] There is a match at the peaks of the O atom N° 13 for the 2s and the O atom N° 26 for the 2s with the Al atom N° 27 for the 3s orbital and the Al atom N° 28 for the 3s orbital and the Al atom N° 35 for the 3s orbital and the Al atom N° 43 for the 3s orbital and the Al atom N° 44 for the 3s orbital.

$[-12.82, -14.78]$ There is a match at the peaks of the O atom N° 13 for the 2s and the O atom N° 26 for the 2s with the Al atom N° 27 for the 3s orbital and the Al atom N° 28 for the 3s orbital and the Al atom N° 35 for the 3s orbital and the Al atom N° 36 for the 3s orbital and the Al atom N° 43 for the 3s orbital and the Al atom N° 44 in the 3s orbital.

$[-3.12, -7.84]$ There is a match at the peaks of the Al atom N° 27 for the 2p and the Al atom N° 28 for the 2d and the Al atom N° 35 for the 3d orbital and the Al atom N° 36 for the 3p orbital and the Al atom N° 43 for the 3p orbital and the Al atom N° 44 for the 3d orbital with the Cu atom N° 11 and 12 and 24 and 25 for the 3d.

We Conclude from our analysis of the PDOS (111) curves that the two interval$[-1.85, -3.60]$; $[-3.12, -7.84]$ have the highest and lowest coinciding orbitals below the Fermi level which indicate a stronger interaction energy at the interface between aluminum and copper oxide.

VI.Conclusion:

The most important results that we reached in this chapter are the following:

Three models were built Al(001)Cu_2O (1 layer of Al and 1 layer of Cu_2O) and Al(001)Cu_2O (2 layer of Al and 2 layer of Cu_2O) with Al(111)Cu_2O (1 layer of Al and 2 layers of Cu_2O), where we studied the adhesion energy between them, and we found that adhesion is achieved in these models because E_{ad} is less than zero.

We compared the two models Al(001)Cu_2O (1 layer of Al and 1 layer of Cu_2O) and Al(001)Cu_2O x(2 layer of Al and 2 layer of Cu_2O) , where we found that the adhesion is better in the model with two layers of Al and two layers of Cu_2O. This explains the effect of the number of layers on the adhesion where the more we increase in a certain number of layers, the better the adhesion.

The nearest neighbors affect the bonding between the atoms (O-Al), as we found that the nearest neighbors distance for the aluminum atom in the two-layer model is better than the one-layer model.

We also compared the two models Al(111)Cu_2O (1 layer of Al and 2 layers of Cu_2O) with Al(001)Cu_2O (2 layers of Al and 2 layers of Cu_2O). Because they have the same number of layers, and we found that the adhesion is good in the Al (111)Cu_2O (1 layer of Al and 2 layers of Cu_2O) model. Then we interpreted this based on an electronic study of the PDOS curves, where we noticed that the number of congruent peaks in the model Al (111) Cu_2O (1 layer of Al and 2

layers of Cu_2O) is more than the number of congruent peaks in the model $Al(001)Cu_2O$ (2 layer of Al and 2 layer of Cu_2O).

Reference:

[1] Bharat Medasani, Igor Vasiliev , " Computational study of the surface properties of aluminum nanoparticles", Surface Science, 603 (2009) 2042–2046.

[2] Vasiliev, I., & Medasani, B."Surface properties of silver and aluminum nanoclusters". Quantum Dots, Particles, and Nanoclusters V, (2008).

[3] Wu, H., Zhang, N., Wang, H., & Hong, S, "Adsorption of CO2 on Cu_2O (111) oxygen-vacancy surface: First-principles study". Chemical Physics Letters, (2013), 568-569, 84–89.

[4] Etghani, S. A., & Nadimi, E , " Investigation of the p-type behavior in Cu2O: An ab initio study, 2015 23rd Iranian Conference on Electrical Engineering.

[5] V.G. Tyuterev, Nathalie Vast," Murnaghan's equation of state for the electronic ground state energy" ,Computational Materials Science 38 (2006) 350–353 .

[6] Fei Pei, Song Wu et al, "Electronic and Optical Properties of Noble Metal Oxides M2O (M = Cu, Ag and Au): First-principles Study", Journal of the Korean Physical Society, Vol. 55, No. 3, September 2009, pp. 1243~1249.

[7] Mazharul M. Islam et al, "Bulk and surface properties of Cu_2O: A first-principles investigation", Journal of Molecular structure:THEOCHEM 903 (2009) 41-48 .

[8] Alejandro Martínez-Ruiz a et al, "First principles calculations of the electronic properties of bulk Cu2O, clean and doped with Ag, Ni, and Zn", Solid State Sciences 5 (2003) 291–295.

[9] R. Gaudoin and W. M. C. Foulkes," Ab initio calculations of bulk moduli and comparison with experiment", PHYSICAL REVIEW B 66, 052104, 2002.

[10] Mariano Forti,"Adhesion Energy of the Fe (BCC)/Magnetite Interface within the DFT approach", Procedia Materials Science 8 (2015) 1066 – 1072.

General conclusion

General conclusion

The perspective of this work, we conducted a study on the interface composed between aluminum and copper oxide with the purpose of constructing a thin film by modeling and simulations using the DFT (Density functional theory). It was implemented in two using SIESTA and Quantum Espresso codes. The focus was on the structural and electronic study of the system.

In this conclusion, we would like to confirm the following key points:

We studied the structural properties that characterize the stability of the aluminum and copper oxide system. The different parameters needed in the calculations were extracted and it was converged on the basis of the minimum values of the system energy, and compared with the theoretical results. We found a good agreement in the values of the lattice parameters and the bulk modulus (which measures the compressibility) for both aluminum and copper oxide Cu_2O.

We constructed the $AlCu_2O$ model with aluminum in the direction of <001> and changed the number of layers. We compared then the two models $AlCu_2O$ (2 layer of Al and 2 layer of Cu2O) and (1 layer of Al and 1 layer of Cu2O) in terms of adhesion energy and found it better in the model $Al(001)Cu_2O$ (2 layer of Al and 2 layer of Cu2O)

We found that the adhesion energy of the model $AlCu_2O(001)$(1 layer of Al and 1 layer of Cu2O) is less than that for the $AlCu_2O(001)$(2 layer of Al and 2 layer of Cu2O). The distance between the aluminum and copper however,remains constant a difference of 0.01A°, which is negligible in atomic dimensions.

We constructed the model $AlCu_2O$(1 layer of Al and 2 layer of Cu2O) with the change in the direction of aluminum <111>, and we found that the adhesion energy of this model is better than the adhesion energy of the model $AlCu_2O(001)$(2 layer of Al and 2 layer of Cu2O).

Regarding the study of electronic properties, we found from our analysis of the PDOS curves of the two models $AlCu_2O(001)$(2 layer of Al and 2 layer of Cu2O) and $AlCu_2O(111)$ (1 layer of Al and 2 layer of Cu2O), that the higher the number of matched orbitals and the lower the Fermi level, the more stronger the bonds between the oxygen and aluminum atoms and the aluminum and copper atoms.

Finally, from our short experiments with the SIESTA and Quantum Espresso programs, these two codes are very useful that allow prediction of all the physical properties of materials.

As a perspective of this work,we hope in the future to model and simulate all other types of copper oxides , taking in consideration the change in the number of layers of the metal and the oxide and the direction of the materials, in the aim to find the number of layers and the direction corresponding to the best adhesion energy thus achieving good physical properties to facilitate experiments in order to guide them for industrial uses.

Abstract:

The work presented in this memory consists of a study of the adhesion aluminum to copper oxide using Quantum Espresso and SIESTA numerical simulation software. We performed calculations based on the ab_initio elementary principles of the structural and electronic properties of Al/Cu2O interface in the DFT famework using generalized gradient approximation (GGA). We constructed the AlCu2O model with the change in the number of layers and the direction of Al then calculate the corresponding adhesion energy, where we found that the adhesion occurs in all the models studied. The results obtained are annotated and interpreted with PDOS curves. Certain the increase in the number of layers improves the adhesion and Al(111)/Cu2O adheres better compared to Al(001)/Cu2O.

Key Words: Adhesion energy, DFT, ab_initio, model, simulation, Aluminum, copper oxide, interface.

الملخص:

العمل المقدم في هذه المذكرة يتكون من دراسة التصاق أكسيد النحاس بالألمنيوم باستعمال برنامج المحاكاة العددية SIESTA وQuantum Espresso,قمنا بحسابات معتمدة على المبادئ الأولية ab_initio للخصائص البنوية والالكترونية لسطح $AlCu_2O$ في اطار نظرية الكثافة التابعية DFT باستخدام تقريب التدرج المعمم GGA . قمنا ببناء النموذج $AlCu_2O$ مع التغيير في عدد الطبقات واتجاه Al ثم حساب طاقة الالتصاق الموافقة ,حيث وجدنا أن الالتصاق يتحقق في جميع النماذج المدروسة . يتم شرح النتائج التي تم الحصول عليها وتفسيرها باستخدام منحنيات PDOS. من المؤكد أن الزيادة في عدد الطبقات يحسن الالتصاق و Al(111)/ Cu2O يلتصق بشكل أفضل مقارنة بـ Al(001)/ Cu2O.

الكلمات المفتاحية: طاقة الالتصاق , DFT, ab_initio , نموذج,محاكاة, المنيوم,أكسيد النحاس,الأسطح البينية .

Résumé:

Le travail présenté dans ce memoire consiste en une étude de l'adhérence de l'aluminium à l'oxyde de cuivre. À l'aide des logiciels de simulation numérique Quantum Espresso et SIESTA, nous avons effectué des calculs basés sur les principes élémentaires ab_initio des propriétés structurelles et électroniques d'interface Al/Cu2O dans le cadre DFT en utilisant l'approximation du gradient généralisé (GGA). Nous avons construit le modèle AlCu2O avec le changement du nombre des couches et de la direction de Al puis calculons l'énergie d'adhésion correspondante, où nous avons constaté que l'adhésion se produit dans tous les modèles étudiés. Les résultats obtenus sont annotés et interprétés avec des courbes PDOS. Certes, l'augmentation du nombre de couches améliore l'adhérence et Al(111)/Cu2O adhère mieux par rapport à Al(001)/Cu2O.

Mots clés: Énergie d'adhésion, DFT, ab_initio, modèle, simulation, aluminium, oxyde de cuivre, interface.